

A Failure Analysis Case Study of the Fluid- Structural Interactions on Trashracks

Rock Island Dam, Powerhouse 1: Units B5-B10

Timothy M. Scheumann

A thesis
submitted in partial fulfillment of the
requirements for the degree of

Master of Science

University of Washington
2012

Committee:

Dr. Per Reinhall (Chair)

Dr. Peter Dahl

Dr. Colin Sandwith

Program Authorized to Offer Degree:
Mechanical Engineering

University of Washington

Abstract

A Failure Analysis Case Study of the Fluid-Structural Interactions on Trashracks

Tim Scheumann

Chair of the Supervisory Committee:

Professor Per Reinhall

Mechanical Engineering

A failure analysis investigation was completed on the trashracks at Powerhouse One of Rock Island Dam. The investigation was part of the overall condition assessment and rehabilitation work being performed at the dam. The trashracks were deemed a faulty system in 2005 when MWH, a contractor for Chelan County PUD, initially inspected the racks. Building on the original work completed by MWH, this project compiled background information and conducted field inspections to evaluate the future reliability of the trashracks. The field inspections identified consistent failures of the diagonal tie rods, discovered cracks in the rackbar welds, and highlighted the noticeable presence of corrosion damage. Though localized failures were identified, a static analysis concluded that the overall structural design was adequate for continued operations. Field tests and a finite element model were compared in a dynamic analysis to ensure the vibration induced stresses did not reach the allowable limit. Ultimately, the trashracks received new diagonal braces constructed from angle iron to replace the failing tie rods. Damaged welds, caused by the propagation of cracks from welding defects, were repaired and the racks were sandblasted to remove corrosion debris and repainted to prevent future degradation.

Table of Contents

List of Figures	4
List of Tables	6
Executive Summary	7
Chapter 1: Introduction	9
Chapter 2: Purpose	10
Chapter 3: Background	12
3.1 <i>History</i>	12
3.2 <i>Trashrack Vibration Literature Review</i>	13
3.3 <i>Rock Island Dam Trashracks</i>	15
3.4 <i>2005 Condition Assessment</i>	17
3.5 <i>Chelan County PUD and University of Washington Partnership</i>	18
3.6 <i>Vocabulary</i>	19
Chapter 4: Failure Analysis Investigation	22
4.1 <i>Field Inspection</i>	22
4.2 <i>Static Structural Analysis</i>	30
4.3 <i>Fatigue Analysis</i>	32
4.4 <i>Vibration Analysis</i>	34
4.5 <i>Corrosion Analysis</i>	36
4.6 <i>Weld Analysis</i>	46
4.7 <i>Design of Diagonal Braces (Tie Rod Replacements)</i>	47
4.8 <i>Rehabilitation Recommendations</i>	51
Chapter 5: Vibration Experiments	55
5.1 <i>Vibration Overview</i>	55
5.2 <i>Experimental Data</i>	55
5.3 <i>Finite Element Model Vibrations</i>	64
5.4 <i>Vibration Experiments Conclusion</i>	68
Chapter 6: Conclusions	70
Bibliography	72

Acknowledgements.....	74
Appendix A: Original Design Specifications.....	75
Appendix B: MWH Evaluation Report (2005).....	84
Appendix C: Calculations.....	87
<i>C.1 Static Structural Calculations</i>	87
<i>C.2 Fatigue Calculations</i>	90
<i>C.3 Vibration Calculations</i>	91
<i>C.4 Welding Calculations</i>	93
<i>C.5 Finite Element Model Results</i>	95
<i>C.6 Tie Rod Replacement Calculations</i>	98
Appendix D: Chelan PUD Painting Specifications	99
Appendix E: Additional Pictures	101

List of Figures

Figure 1: Plan view of Rock Island Dam. The location of the trashracks is identified by the yellow line.	15
Figure 2: Plan view of Powerhouse One at Rock Island Dam. The trashracks are identified by the yellow box.	16
Figure 3: Computer model of the original B5 through B10 trashracks.	17
Figure 4: Steel framed trashrack with vertical steel rackbars.	23
Figure 5: Steel framed trashrack with vertical wood rackbars.	23
Figure 6: Each trashrack should have four diagonal tie rods to provide stability when moving the 7,000 pound structures. This picture is an example of one rack which is missing three of the tie rods (locations identified in yellow) and the one remaining rod was very loose.	24
Figure 7: This picture shows a common instance of tubercles as found on the trashracks (right) and the pits which had formed under the tubercles (left).	25
Figure 8: The first round of magnetic particle testing was performed through the paint. The grey powder serves as a strong indication that there is a crack in the weld. This proved to be true after grinding into the weld.	27
Figure 9: Here is an example of one of the inclusions discovered in the welds. Inclusions are major stress risers in the welds.	27
Figure 10: Magnetic particle testing was performed a second time after the trashracks were sandblasted. Red powder was used here to identify the crack.	28
Figure 11: The steel trashracks are grey after sandblasting. This operation removes all the paint which exposes the structure for a thorough investigation and prepares it for painting. The blue tape was used to identify cracks.	28
Figure 12: The protective layer of paint was applied unevenly and dripped in many locations. This was likely do to a rushed application process which resulted in uneven layers and was accentuated by the fact that it was applied at an improper ambient temperature.	29
Figure 13: The new paint job was peeling along the guide bars before the trashracks entered the water. This was likely caused by the fabricators stacking the trashracks before the paint was fully cured.	29
Figure 14: Front view of the trashrack modeled in ANSYS with a static head of 5 ft. The maximum Von Mises stress is 13.8 ksi.	31
Figure 15: Convergence plot for the maximum Von Mises stress on the trashrack finite element model.	32
Figure 16: A grouping of individual tubercles.	37
Figure 17: Widespread growth of tubercles.	38
Figure 18: Corrosion damage under a few individual tubercles.	38
Figure 19: Corrosion damage under a surface covered with tubercles.	39
Figure 20: Corrosion deposits along a welded joint.	39
Figure 21: Corrosion damage after the tubercles have been removed from the weld.	40
Figure 22: Erosion corrosion damage of leading edge.	42
Figure 23: Corrosion rate versus velocity for steel in fresh water.	43
Figure 24: Example of biological growth.	44
Figure 25: Galvanic corrosion due to coupling of steel bolt to the bronze spring.	45
Figure 26: Fretting corrosion evident on the steel tie rod.	46

Figure 27: General response of the accelerometer during a sweep in flow rate through the trashrack. Vibrations are plotted in the direction of flow, in the lateral direction, and in the vertical direction.....	57
Figure 28: Trashrack vibration response in the direction of flow. The spectrogram plot on the top highlights the dominant frequencies while the bottom plot provides the general response of the accelerometer and the corresponding flow rate. Spectrogram data is presented in decibels and is normalized according to the color bar on the right.....	58
Figure 29: Trashrack vibration response in the lateral direction. The spectrogram plot on the top highlights the dominant frequencies while the bottom plot provides the general response of the accelerometer and the corresponding flow rate. Spectrogram data is presented in decibels and is normalized according to the color bar on the right.....	60
Figure 30: Trashrack vibration response in the vertical direction. The spectrogram plot on the top highlights the dominant frequencies while the bottom plot provides the general response of the accelerometer and the corresponding flow rate. Spectrogram data is presented in decibels and is normalized according to the color bar on the right.....	62
Figure 31: Steady state fast Fourier transform plots at varying flow rates. The power density spectrum for the response data is plotted in units of $(m/s^2)^2/Hz$	63
Figure 32: Finite element model vibration mode 5. This is the first resonant frequency of the 57 inch rackbars and occurs at 33.6 Hz.....	65
Figure 33: Finite element model vibration mode 13. This is the first resonant frequency of the 28.5 inch rackbars and occurs at 79.7 Hz.	67
Figure 34: Front view of the trashrack modeled in ANSYS with a differential hydrostatic head of 5 feet. The maximum Von Mises stress is 13.8 ksi.....	96
Figure 35: Rear view of the trashrack in ANSYS. The maximum stress (13.8 ksi) occurs at the center of the horizontal structural channels.	96
Figure 36: Front view of the trashrack in ANSYS displaying the deformation due to the applied load. The maximum deformation is just over 0.2 inches.	97
Figure 37: Front and side views of original trashrack model.	101
Figure 38: Front view of the original trashrack with steel rackbars while hanging from the gantry crane. Three of the four diagonal tie rods are missing.....	101
Figure 39: Front view of a original trashrack with wood rackbars. The structural supports and diagonal tie rods are identical for the wood rackbar and steel rackbar trashracks.....	102
Figure 40: Rehabilitated trashrack demonstrating the new diagonal braces. The angle iron braces were installed with the elbow of the angle pointing directly into the flow.	102
Figure 41: Rehabilitated trashrack. The new diagonal braces were installed and the structure was sandblasted and painted black. Tim Scheumann is standing in front of the trashrack.	103

List of Tables

Table 1: Relevant vocabulary.....	20
Table 2: Static structural calculations summary.	30
Table 3: Parameters for Marin’s fatigue endurance limit equation.	33
Table 4: Parameters of Levin's rackbar natural frequency equation.....	34
Table 5: Parameters of Strouhal's forcing frequency equation.	35
Table 6: Vibration calculations summary.	36
Table 7: Coefficient of drag, drag force, shear stress, and bending force for the original rod, the potential 1.25" rod and the potential two inch angle.....	49
Table 8: Vortex shedding frequency according to the Strouhal number.	50
Table 9: Comparison of section modulus values for the rods and the angle iron braces.	50
Table 10: Harmonic frequencies and mode shapes of the trashrack according to the finite element model modal analysis system. The rackbar vibrations are identified in italics.	64
Table 11: Parameters for structural calculations.	87
Table 12: Static structural calculations for the rackbars of the trashrack at varying loads and corrosion.	88
Table 13: Static structural calculations for the top beam of a trashrack at varying loads and corrosion.	89
Table 14: Static structural calculations for the middle beam of the trashrack at varying loads and corrosion.	89
Table 15: Endurance limit calculations for A30 steel.	90
Table 16: Gross and net flow dimensions for a single trashrack.....	91
Table 17: Net flow area for one intake bay at the turbine.	91
Table 18: Rackbar vibration forcing frequency calculations for turbines B5 and B6.....	92
Table 19: Rackbar vibration forcing frequency for turbines B7 through B10.	92
Table 20: Rackbar natural frequency for units B5 through B10.....	93
Table 21: Vortex shedding vibration calculation summary.	93
Table 22: Weld analysis parameters for center horizontal channel.	94
Table 23: Bending and shear stress calculations for the rods and the angle diagonal braces.	98
Table 24: Vortex shedding frequency according to the Strouhal number.....	98

Executive Summary

For the past decade, Chelan County Public Utility District has been moving forward with a major modernization project of Powerhouse One at Rock Island Dam. This powerhouse was originally installed in the 1930s and was expanded in the 1950s. In addition to increasing the efficiency of electricity generation, the District plans to repair or replace all aging systems at Powerhouse One. Based on a 2005 condition assessment performed by MWH, the trashracks were one of the faulty systems requiring attention. Accordingly, a failure analysis investigation was performed on the Powerhouse One trashracks at Rock Island Dam.

The investigation was completed as a master's thesis project through the Mechanical Engineering Department at the University of Washington in collaboration with Chelan County PUD. It was designed to survey the current condition of the trashracks to determine whether repairs could return the trashracks to a safely, reliable state of operation. The second part of the project was to provide the District with a list of appropriate rehabilitation recommendations, assuming that repairs and modifications would be more cost effective than redesigning and replacing the trashracks entirely. At the start of the project, the management team at Chelan County PUD speculated that vortex shedding vibration frequencies from the flow of the river was exciting resonant mode shapes on the trashracks which was causing structural fractures.

After conducting various rounds of field inspections, it was determined that the trashracks were not as damaged as originally thought. Though the diagonal tie rods were consistently failing, the only other issues identified by the study were cracks in some welds and corrosion damage. From that point forward, the failure analysis project shifted focus to validate the strength of the existing design while also developing a plan of action for the parts that needed to be repaired.

Based on the structural analysis and the corresponding rehabilitation recommendations, the trashracks were repaired in 2011. New diagonal braces, designed to reduce lateral vibrations due to vortex shedding, were installed to replace the original tie rods. Defective welds, which were identified by cracks that propagated to the surface from inclusions and undercut within the welds, were ground out and replaced. Finally, the trashracks were

sandblasted to remove corrosion deposits and repainted prevent future degradation of the steel.

Experimental data of the trashrack vibrations was also gathered during the case study. The results of the experimental data were compared to vibration calculations and a finite element model to determine the significance of lateral rackbar vibrations. The conclusions indicate that the vortex shedding from the flow around the rackbars does excite vibration mode shapes at natural frequencies of 35 Hz and 70 Hz. However, the amplitude of the vibrations was determined to be low enough to not cause structural damage to the trashracks during the first 60 years of operation. It follows that there is verifiable evidence that the modified trashracks will provide service for the next 40 years.

Chapter 1: Introduction

A failure analysis investigation was performed on the B5-B10 trashracks at Powerhouse One of Rock Island Dam. This was a collaborative project between Chelan County PUD and the Mechanical Engineering Department of the University of Washington. The trashracks were analyzed by applied theoretical calculations, finite element analysis models, and physical instrumentation.

A list of rehabilitation recommendations and maintenance instructions was developed from the investigation. The purpose of these recommendations is to obtain another 40 years of service from the modified trashrack design.

Though the trashracks were operating in a harsh marine environment for over 60 years, only a few modifications were necessary for continued operations because the structures were fundamentally adequate. Welds were repaired where defects in the original welding procedure led to vibration and fatigue cracks. Two new braces replaced the four diagonal tie rods while maintaining the required lateral stability. A complete overhaul of the protective paint, following a sandblasting procedure, provided the necessary corrosion protection. New wood and fasteners were installed because the original pieces could not be reused. Finally, a list of maintenance instructions was provided to Chelan County PUD to ensure the trashracks reach the expected 40-year life.

Chapter 2: Purpose

Chelan County PUD and MWH discovered that components of the trashracks at Rock Island Dam were failing when they conducted the condition assessment of Powerhouse One. Visual inspection of the structures revealed that the main concerns were the vertically oriented rackbars and the diagonal tie rods. The rackbars showed signs of cracks near or through the welds. None of the cracks on the B9 trashracks had led to complete failures, but divers have reported the existence of through material cracks in other locations. The tie rods were either fracturing near their connection points or fretting to the point of failure. None of the 60 year old trashracks in unit B9 had functioning tie rods. In addition, a set of new tie rods, which were installed in unit B10 three years ago, were missing or not supporting a load.

It was hypothesized that the flow of water into the turbine caused the rackbars and tie rods of the trashracks to vibrate near the natural frequencies of the system which initiated the failures. These vibration issues, as well as other structural issues including corrosion, fatigue, and static load stresses, were the motivation behind the failure analysis investigation.

The purpose of this study was to properly categorize the trashrack failures and recommend a method to rehabilitate the structures for another 40 years of use. If not repaired, fractured rackbars and tie rods could flow into the scroll case causing damage to the turbine. Additionally, the effectiveness of the trashrack is compromised as holes appear in the metal grid. The lack of diagonal bracing also increases the possibility of misalignment during the re-racking process, or worse, lifting a trashrack with one gantry hook and tearing it apart 60 feet underwater.

The scope of the project was limited to the structural investigation. Operational handling of the trashracks and the cleaning procedure, also known as raking, were not examined because these were not deemed critical issues. Additionally, the hydraulic performance and rackbar spacing were not examined because the current differential head loss of less than one foot across a clean trashrack was within the acceptable range and 12 inch rackbar spacing is very common for Kaplan turbines.

Tim Scheumann conducted the *Failure Analysis Case Study of the Fluid-Structural Interactions on Trashracks* as his Mechanical Engineering Master's thesis project at the University of Washington in conjunction with Chelan County Public Utility District (PUD). He gathered background information on the trashracks, conducted field inspections, investigated several modes of failure, and built a finite element model to validate his conclusions. In addition, experimental data was gathered to further examine the vibration characteristics of the trashracks.

Chapter 3: Background

The Background Section presents an assortment of information necessary to understand the trashrack failure analysis investigation. A general discussion about Rock Island Dam is offered to provide context for the project and a literature review examines the engineering hurdles associated with trashrack designs. Vocabulary pertinent to the thesis paper is presented at the end of the chapter.

3.1 History

Hydropower has been the driving source of fame and growth along the Columbia River, and much of the Pacific Northwest for nearly a century. There was once a time when the river raged untamed, but that era has since been marked as the age of untapped potential. Theodore Roosevelt was one of the first major advocates of constructing dams along the Columbia River to enhance navigation, provide flood control, and most notably, generate cheap hydroelectric power for the region. His leadership in the early 20th century eventually led to the development of 14 dams on the mainstream Columbia and over 270 in the Columbia River Basin.¹

Rock Island Dam was the first dam constructed on the Columbia River. Stone and Webster Engineering Corporation, the managing corporation for Puget Sound Power and Light, completed the dam in 1933. Four turbines were commissioned that year, but these were just the first phase of a long term development plan. Six additional turbines were added to the original powerhouse in 1953, and a second powerhouse with eight turbines was added in 1979.²

Chelan County PUD was operating Rock Island Dam in the 1950s when the second expansion phase was initiated. The six turbines and generators added to Powerhouse One were identified as units B5 through B10. Each of these units is rated for a maximum generating capacity of 22.5 Megawatts. The increased generating capacity was added to meet an increasing demand for electricity in the region. Though the entire expansion project is an interesting topic by itself, it is not the subject of this paper. Rather, the

¹ (Northwest Power and Conservation Council)

² (Chelan County PUD)

expansion project of the 1950s is of interest today because a new set of trashracks was designed for this bank of turbines.

Trashracks are large steel or wooden structures which prevent debris in a river from entering the scroll case of a turbine. From a basic perspective, they are very large filters. Trashracks are assembled by attaching a series of vertical rackbars, serving as the straining mechanism, to a structural frame. The frame is usually constrained by the concrete structure of a dam. Debris in the flow of the river can have a negative impact on the turbines by physically damaging the turbines or by decreasing the generating efficiency. Trashracks must be designed to withstand the accumulation of debris along the face of the rackbars while operating with minimal fluid flow losses. The accumulation of debris and the flow losses are typically expressed by differential head in units of feet.

3.2 Trashrack Vibration Literature Review

Hydroelectric facilities require the seamless integration of an array of systems. Since the late 1800s, engineers have worked to improve the design and efficiency of the original dams which were closer to large scale fabrication projects than precisely designed power plants.³ Trashrack designs came under specific scrutiny in the 1960s and 1970s through the work of Par Levin and Lloyd Sell. These applied researchers characterized the vibration of rackbars on the trashracks and defined four significant aspects to consider when designing trashracks.

Sell specified that trashrack designers must consider the following four general features: differential design head; trashrack bar spacing; head loss; and vibration.⁴ Differential design head, rackbar spacing, and head losses can each be easily defined. These parameters are based on static or quasi-static measurements, and relatively few variables complicate a close match between the design and the actual operation. However, the vibration response of trashracks, and specifically rackbars, is not an easily quantified problem. It therefore follows that Levin's research is important because he focused on improving the stability of trashracks to combat vibration failures.

³ (Bureau of Reclamation, 2009)

⁴ (Sell, 1971)

Vibrations on the trashrack are a major focus of this thesis. While the first three trashrack design features were explored in this case study, it was much easier to validate that they were indeed properly considered and not an operational issue. The vibrations, in contrast, present a much more complicated study, which is why Levin's vibration studies are important. A couple decades before Levin was publishing his research, Timoshenko characterized the natural frequency of beams in a vacuum. Levin applied Timoshenko's results to trashracks by incorporating the mass damping effects of water on the rackbars.⁵ He was thus able to define the natural frequency of the rackbars and compare this frequency to the forcing frequency due to the approaching fluid flow.

Strouhal forcing frequency functions for beams in fluid flow had been around for over half a century before Levin started working on his trashrack research. Minor research was conducted to obtain a linear relationship of the Strouhal number to the aspect ratio of rackbars, but most of the work was put toward developing a simple representation of the natural frequency of vibrations. This equation will be presented later, but it should be known that these vibrations are due to either Karman vortices or impinging leading-edge vortices. Though exact resonance is met when the forcing frequency reaches the natural frequency, it is recommended that the velocity of the incoming fluid be limited to that which causes at most 40% of the resonant frequency. This is due to the considerable damping effect of the water which results in resonance over a wide frequency range.⁶

Vortex shedding characteristics are determined largely by the aspect ratio, but are also related to other factors. Rounded edges and the impact angle of the fluid have noteworthy effects on the vibration excitation. Specifically, streamlined rackbars and rackbars operating at a fluid flow angle of incidence greater than ten degrees are subject to vibrations of higher magnitude than square edged rackbars and rackbars oriented nearly parallel to oncoming flow.^{7,8} Streamlined bars are effective at reducing head losses across trashracks, but they suffer from impinging leading-edge vortices. The rackbars in this investigation have an aspect ratio of eight which places them well within the large aspect ratio range. The fluid flow angle of incidence is significant because the pressure differential on opposite sides of the rackbars creates "effective lift" causing the bars to twist back and

⁵ (Levin, 1967)

⁶ (Fortey & Tiry, May 1972)

⁷ (Naudashcher & Wang, 1993)

⁸ (Nguyen & Naudascher, 1991)

forth. This phenomenon is initiated earlier when the rackbar edges are rounded because the streamlines around the structure reattach quicker.

The background research on rackbar vibrations can be summarized by the conclusion that vibrations are at a minimum when large aspect ratio rackbars with square edges are oriented directly in line with the flow. Additionally, the vibrations can be reduced by decreasing the unsupported length of each rackbar. These vibration reduction techniques do increase the head losses so there is always a tradeoff which must be explored.

3.3 *Rock Island Dam Trashracks*

Rock Island Dam is located in central Washington, approximately ten miles south of Wenatchee. It spans the Columbia River in a wide, but shallow stretch of river. It was the first dam constructed on the river and has been through two additional expansion phases. Rock Island Dam has two power plants; one on the north side of the river with a generating capacity of 213 megawatts and one on the south side of the river with a generating capacity of 410 megawatts. The trashracks of interest for this failure analysis investigation are located in Powerhouse One, which is highlighted in the plan view of Figure 1 and are located on the north side of the river. An elevation view is provided in Figure 2 to highlight the specific location of the trashracks.



Figure 1: Plan view of Rock Island Dam. The location of the trashracks is identified by the yellow line.

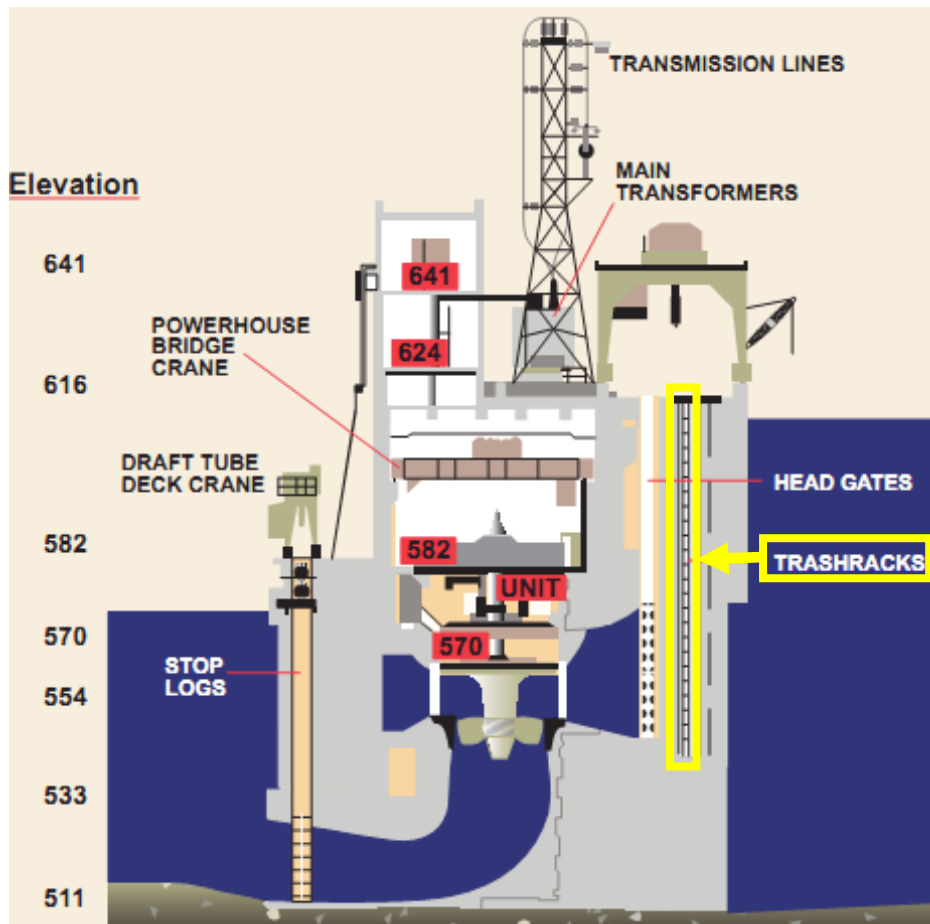


Figure 2: Plan view of Powerhouse One at Rock Island Dam. The trashracks are identified by the yellow box.

The trashracks for units B5 through B10 are the focus of this failure analysis project. Each unit has three intake bays leading to the scroll case. There are 18 trashracks per unit which are stacked six high per intake bay. The bottom three trashracks in each bay have steel rackbars while the top three trashracks have wood rackbars. These trashracks are approximately 17 feet wide by 11 feet high and weigh 7,000 pounds. The center to center spacing for all rackbars is 12 inches, but the steel bars have a frontal width of 0.5 inches and the wood rackbars have a frontal width of eight inches.

Stone and Webster Corporation designed the trashracks and W.H. Reller performed the fabrication. The shop drawings from W.H. Reller for 54 trashracks with steel rackbars and 54 trashracks with wood rackbars are from 1951. Units B5 through B10 were commissioned between 1952 and 1953. A copy of the original Invitation for Bids for the fabrication work is included in Appendix A. Figure 3 portrays a computer model of the B5 through B10 trashracks.

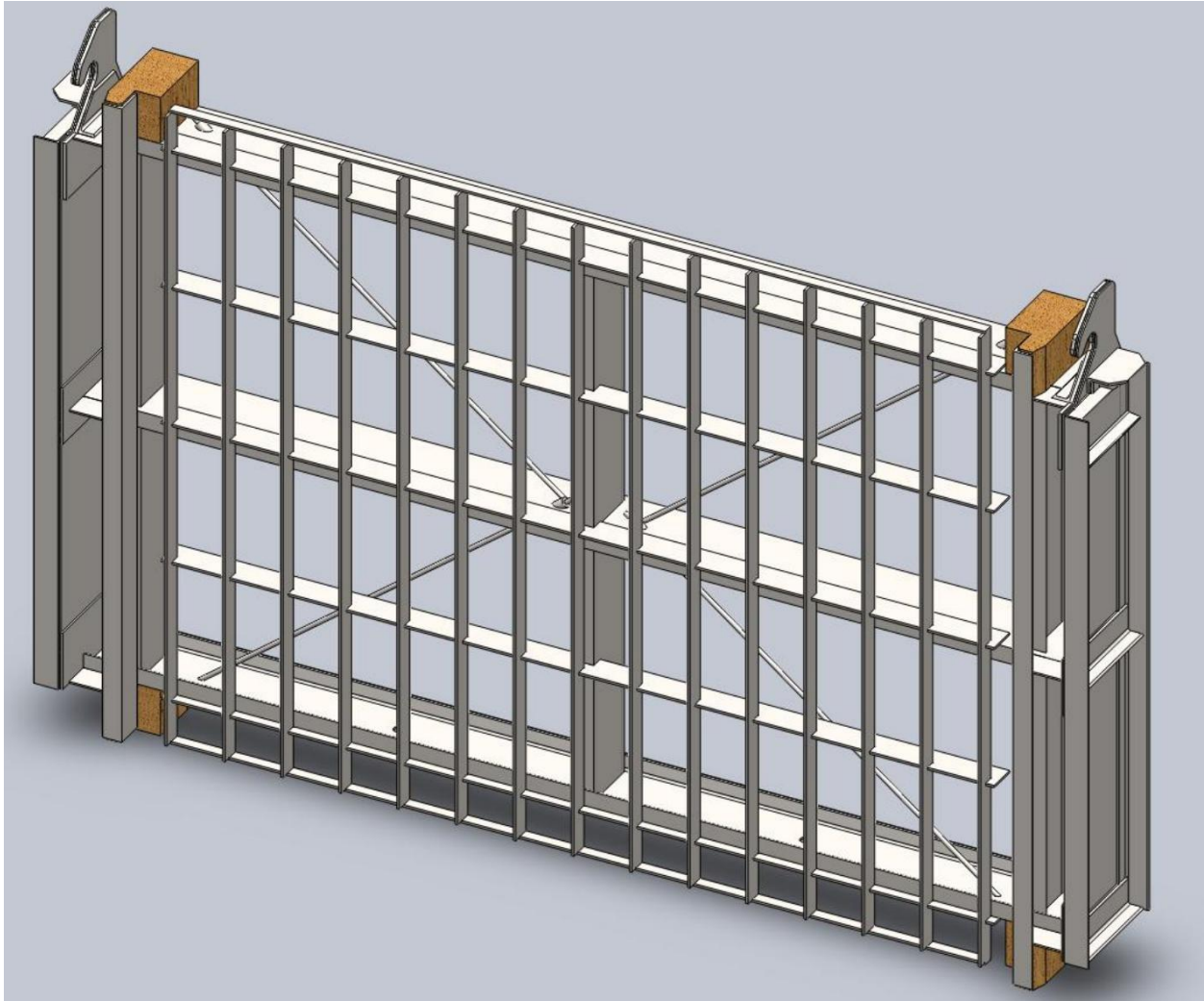


Figure 3: Computer model of the original B5 through B10 trashracks.

3.4 2005 Condition Assessment

There is no documented information on the condition or performance of the trashracks between commissioning in the mid-1950s and the B10 condition assessment in the mid-2000s. It is thus assumed that the current trashracks are original and have not received any major modifications. The paint appears to be the original coal tar epoxy. The wood rackbars appear to be the original creosote soaked Douglas fir timbers.

The most recent trashrack information is available from a MWH report. MWH is a consulting company which was hired by Chelan County PUD to assist the District in conducting a

condition assessment of Powerhouse One at Rock Island Dam. Their 2005 trashrack evaluation report provided the following list of conclusions:

1. The 12 inch rackbar spacing is acceptable for the trashracks.
2. The trashracks can adequately support a differential head of five feet but should be strengthened in the near future to support a load of ten feet which is commonly used for new trashrack designs.
3. The unsupported length of the rackbars should be reduced to increase the vibrational factor of safety for long term operations.
4. No hydraulic modifications are necessary.
5. Trashracks in at least two other intake bays should be inspected to verify the conclusions of the initial investigation.
6. New trashracks could be designed and placed on the outermost wall of the dam to increase the ease of cleaning and handling.

Originally, the MWH investigation was projected to be phase one of a two phase project. This first phase initiated the inspection and assessment of the trashracks while the second phase was going to begin a rehabilitation study if it was determined that new or repaired trashracks were necessary. However, phase two was not conducted by MWH, but rather commenced when Tim Scheumann started the Failure Analysis Case Study of the Fluid-Structural Interactions on Trashracks in the fall of 2010. Scheumann and MWH shared common ground on the condition assessment (phase one), though Scheumann's investigation also provided a list of rehabilitation recommendations to extend the operational life of the trashracks another 40 years (phase two). Refer to Appendix B for the Executive Summary of the 2005 report from MWH.

3.5 Chelan County PUD and University of Washington Partnership

The *Failure Analysis Case Study of the Fluid-Structural Interactions on Trashracks* was a joint investigation between Chelan County PUD and the University of Washington. Tim Scheumann had completed an internship at Rock Island Dam in the summer of 2010 and was looking for a thesis project for the start of his master's degree at the University of Washington. Due to his interest in an industry applied project, he asked his supervisor at the dam, Brett Bickford, if he could work on a project for the District as his master's thesis

project. Bickford was open to the idea and helped Scheumann identify potential projects while navigating the managerial guidelines to set up the joint project.

After a few months of negotiations between Chelan County PUD and the University of Washington, Scheumann's thesis project was approved. Bickford remained the primary contact from the District and Dr. Per Reinhall, the Chair of the Mechanical Engineering Department, was selected as Tim's thesis advisor at the University. Dr. Per Reinhall has an interest, among other areas, in fluid-induced vibrations and finite element modeling. His interests aligned well with the vibration concerns of the trashrack and the need to validate decisions with a computer model.

Scheumann began working on the project in the spring of 2011 after the project proposal, outlined by the scope of work and a budget from the District, was approved in the winter of 2011. He spent the summer of 2011 at Rock Island Dam before returning to Seattle for the 2011-2012 school year. A list of Rehabilitation Recommendations was provided to Bickford and Chelan County PUD in November 2011.

3.6 Vocabulary

Table 1 provides definitions to many of the commonly used words in this document. This list describes some common parts of a dam as well as the vocabulary specific to Chelan County PUD.

Table 1: Relevant vocabulary.

Term	Description
ANSYS	ANSYS was the finite element modeling software package used for the trashrack failure analysis project.
B units	Chelan County PUD operates two powerhouses at Rock Island Dam, one powerhouse at Rocky Reach Dam, and one powerhouse at Chelan Falls Dam. The bank of units within each powerhouse is categorized internally by a letter of the alphabet. Powerhouse One houses the B units.
Chelan County PUD	Chelan County Public Utility District provides electric, water, and wastewater services for Chelan County. It is a public utility in central Washington organized as a nonprofit municipal corporation and is customer owned. The PUD operates three dams, including Rock Island Dam.
Differential head	Differential head is the term used at hydroelectric facilities to express pressure head. It serves two purposes at the dam. First, it is the representation of pressure available to convert mechanical energy to electrical energy. Second, it is a way to express the hydrodynamic loading on the trashracks from the flow of the river.
Generator	Generators are devices which convert mechanical energy to electrical energy. The generators at Rock Island Dam are coupled to the turbines by a large shaft. The flow of the Columbia River causes the turbine to rotate, which in turn spins the generator to produce electricity.
Intake bay	The intake bays are the openings in the dam which direct the flow of the river into the scroll case. There are three intake bays for each turbine at Rock Island Dam.
Powerhouse One	Powerhouse One is the original powerhouse installed at Rock Island Dam. Four turbines (and one house unit) were installed in 1933 and six additional turbines were installed in 1953. The trashracks under investigation were part of the expansion project of the early 1950s. This powerhouse has a generating capacity of 212 megawatts. ⁹
Rackbar	Rackbars are vertically oriented members which serve as the straining mechanism on trashracks. In this project, the rackbars on the lower trashracks are metal and the rackbars on the upper trashracks are wood.
Rock Island Dam	Rock Island Dam is a hydroelectric dam on the Columbia River. It is operated by Chelan County PUD and is located approximately 10 miles south of Wenatchee, WA. It has a generating capacity of 622.5 megawatts. ¹⁰

⁹ (Columbia Basin Research, 2012)

¹⁰ (Columbia Basin Research, 2012)

Table 1 (continued): Relevant vocabulary, page 2.

Term	Description
Scroll case	The scroll case is the spiral cavity directing the flow of the river from the intake bays into the turbine.
The District	The District is the shorthand name for Chelan County PUD. Most employees refer to the entity as The District.
Trashrack	Trashracks are metal or wooden structures designed to prevent debris from entering an intake. In this project, trashracks consist of a steel frame which supports metal or wood rackbars to stop large water-borne debris from entering the turbines at Rock Island Dam.
Tubercles	Tubercles are small mounds of corrosion deposits which form over autocatalytic pits.
Turbine	A turbine is a rotating mechanical device designed to extract energy from a flowing fluid. The turbines at Powerhouse One of Rock Island Dam are vertically oriented Kaplan turbines operating under a differential head of approximately 40 feet. The trashracks at the dam are designed to protect the expensive turbines from structural damage.
Unit	A unit is the coupled system of turbine and generator.
Units B5 and B6	Units B5 and B6 are located near the center of Powerhouse One. They extend from an elevation of 541.5 feet to 609.5 feet and are positioned 5.75 feet behind a vertical concrete breast wall which extends from the deck down to elevation 574 feet.
Units B7 through B10	Units B7 through B10 are located at the south end of Powerhouse One. These units historically accumulate more trash than the rest of the units because they are located close to the center spill gates. They extend from an elevation of 541.5 feet to 609.5 feet and are positioned 5.75 feet behind a vertical concrete breast wall which extends from the deck down to an elevation of 580 feet. The trashracks in unit B9 and the north slot of B10 were removed for the field inspections. The vibration tests were performed in the north slot of B10.

Chapter 4: Failure Analysis Investigation

The failure analysis investigation was a multi-stage project. The main parts of the process included the background research, the field inspections, the applied calculations, and the finite element model. These steps were performed between the April 2011 and October 2011. Information from this analysis was used to provide Chelan County PUD with a list of rehabilitation recommendations at the start of November 2011. This chapter of the thesis includes all the information necessary to justify the list of repairs which are discussed at the end of this chapter. The presentation of the experimental data is presented in the next chapter. The modes of failure which are examined in this chapter are not presented in any particular order.

The trashracks were fabricated in 1952 with ASTM A30 steel. This steel has a yield strength of 30 ksi and an ultimate tensile strength of 55 ksi. These were the material properties used for the structural calculations in the project. ASTM A30 steel was withdrawn from the ASTM standards in 1964.¹¹

4.1 *Field Inspection*

Field inspections were performed over the course of six months and provided the most concrete data for the project. The opportunity to visually examine the trashracks for signs of failure guided many of the analysis decisions. Ultimately, the lack of visual fractures was the most significant piece of evidence that the sixty year old trashracks would be able to continue to operate for another forty years with minimal modifications.

Trashracks from unit B9 were first removed from the water in May 2011. All eighteen racks were removed over the course of a couple of days and placed in the "boneyard" at Rock Island Dam. Figure 4 and Figure 5 depict the general condition of the steel framed racks with steel rackbars and wood rackbars as they were removed from the operating slots. The paint was originally orange, but sludge from the river and the growth of micro-organisms tainted the once vibrant color.

¹¹ (American Society for Testing Materials, 1953)



Figure 4: Steel framed trashrack with vertical steel rackbars.



Figure 5: Steel framed trashrack with vertical wood rackbars.

At the beginning of the project, the management team at Rock Island Dam, based on information from the diving crew, expressed concern that the rackbars were fracturing near the welded connections to the structural cross members. Based on this information, it was surprising to discover that none of the rackbars on the nine steel trashracks were cracked. Most of the tie rods were broken and there was a lot of corrosion damage, but the lack of damaged rackbars represented a major communication discrepancy. This was the first step toward solidifying the fact that the design of the existing trashracks was sufficient for continued operations.

Since there were no fractured rackbars, the broken or missing tie rods and corrosion damage were the most significant aspects to examine. An example of missing tie rods is available in Figure 6. It was clear that the existing tie rod design was not structurally sufficient for the 8,000 or more cubic feet per second flow rate into the turbine. Removing the existing 7/8 inch round tie rods and replacing them with a new diagonal bracing system would eventually be one of the most significant design recommendations for the trashrack rehabilitation project.



Figure 6: Each trashrack should have four diagonal tie rods to provide stability when moving the 7,000 pound structures. This picture is an example of one rack which is missing three of the tie rods (locations identified in yellow) and the one remaining rod was very loose.

Wide spread corrosion damage was the second most noticeable issue on the trashracks. Water had penetrated the coal tar epoxy coating across the trashracks, with severe concentrations found in the areas with higher flow. The most noticeable corrosion mechanism was the widespread existence of tubercles. Tubercles formed under the protective layer of paint and created pits which deposited the gouged materials as bubbles on the surface of the racks. These material deposits were easily removed with a hammer and a steel brush. Figure 7 provides an example of the tubercles found on the trashracks. When the trashracks were fresh out of the water, the loose material could be wiped cleanly out of the pit. Weeks later, after the trashrack had completely dried, the tubercles flaked off when struck with a hammer and the remaining deposits were essentially powder. Erosion corrosion was also prevalent on the leading edge of the rackbars. Pictures of the corrosion damage will be presented in the Corrosion Analysis Section (4.5).



Figure 7: This picture shows a common instance of tubercles as found on the trashracks (right) and the pits which had formed under the tubercles (left).

Micro-organisms, mainly sponge like algae, were found on the ends of the trashracks. Growth of this nature only formed in areas of low flow and was easily removed. They had not penetrated the paint and did not appear to have been related to the corrosion problem. The specific nature of the micro-organisms was not investigated because it did not appear to have a negative effect on the trashracks.

Beyond the missing tie rods and the corrosion damage, there were no other critical structural issues observed during the first inspection on May 2011. The exposed surfaces of the fasteners were badly corroded, but none were missing and they were all supporting the required loads. A few of the leaf springs on the front edge of the racking rails were plastically compressed, but they still served the required function of assisting in the alignment of the trashrack while stacking. The wood rackbars and support blocks were quite weathered, but there were no soft spots in the wood and they were still structurally sound.

Additional field inspections were conducted during the summer of 2011 to explore trashracks beyond unit B9. First, an underwater camera was used in the north intake slot for unit B10. The camera could identify missing rackbars, but this method was not useful for checking cracks along the rackbar connections or assessing corrosion damage. Since the camera did not yield the desired information, the dive crew inspected the B10 trashracks while removing debris as part of the annual cleaning process. The divers were not able to thoroughly check for cracks at the rackbar connections, but they did identify that nearly half of the diagonal tie rods in the north, middle, and south intake bays of unit B10 were missing. This meant that many of the tie rods were breaking within the first few years of operation because these rods were replaced in 2008. Many of the remaining tie rods that were still connected were noticeably loose. The six trashracks stacked in the north slot of B10 were eventually lifted out of the water to check for cracks along the rackbars. However, similar to all the racks from B9, no clear fractures were found.

Cracks in the trashracks were not identified until an initial round of exploratory magnetic particle (MT) testing was conducted. The District mechanics cleaned the welds with a pressure washer, scrapped off the remaining corrosion deposits with a steel brush, and then checked all the welds on two trashracks for indications of cracks through the old paint. They found indications of 20 cracks on the two trashracks inspected. An example of the type of indications found can be seen in Figure 8. To determine whether these indications of cracks were actually cracks or voids, the mechanics then ground into a number of the welds. This investigation, which revealed repeated instances of inclusions and undercut in the welds, quickly became the most significant source of information for the project. Figure 9 provides an example of the type of inclusions found in the welds.



Figure 8: The first round of magnetic particle testing was performed through the paint. The grey powder serves as a strong indication that there is a crack in the weld. This proved to be true after grinding into the weld.



Figure 9: Here is an example of one of the inclusions discovered in the welds. Inclusions are major stress risers in the welds.

The final round of structural field inspections was conducted at the fabrication shop after the trashracks had been sandblasted. Removal of the paint was necessary prior to repainting and essential to improve the accuracy of the MT test results. All of the B9 trashracks showed indications of cracks during the final inspection; the worst rack produced 27 indications of cracks. Figure 10 shows an example of an indication produced by the District inspector. The next picture, Figure 11, shows an entire trashrack in the sandblasted state.

As a side note, it is important to recognize that the MT testing produces indications of cracks and is not an absolute method for locating cracks. However, it is a very cost effective method for detecting virtually all cracks on simple geometries.



Figure 10: Magnetic particle testing was performed a second time after the trashracks were sandblasted. Red powder was used here to identify the crack.

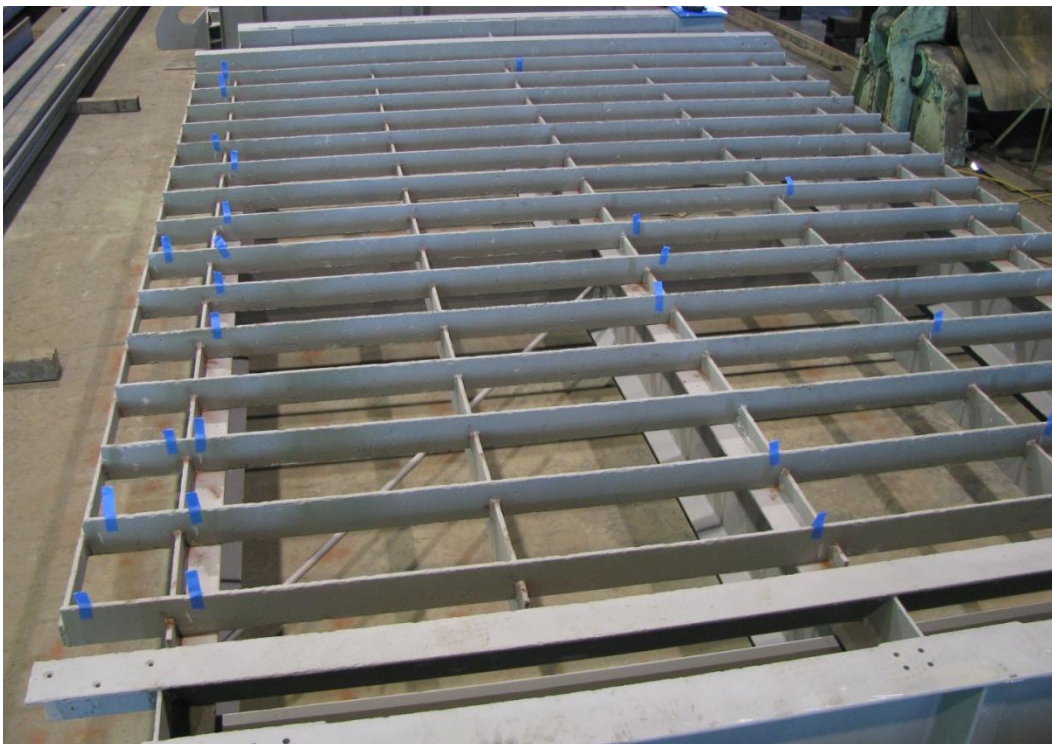


Figure 11: The steel trashracks are grey after sandblasting. This operation removes all the paint which exposes the structure for a thorough investigation and prepares it for painting. The blue tape was used to identify cracks.

The MT tests which followed the sandblasting operation were the last official inspections performed. However, the final state of the trashracks, prior to unit commissioning, was observed as the trashracks were deployed into the water. There are two main points to emphasize about the repaired state of the trashracks. First, the structural repairs were conducted according to the specifications provided and were approved by the District. Second, the protective coating could have been applied better. Figure 12 and Figure 13 demonstrate the imperfections in the paint. There are many areas which suggest the paint was not applied at the proper ambient temperature and that it was applied too thick because paint drips and areas with obvious uneven application layers were common. Additionally, the trashracks were likely stacked before the paint had fully dried which resulted in peeling along the guide rails. Fortunately, the structural repairs are more important to the upcoming 40 years of operation than the condition of the final coating.



Figure 12: The protective layer of paint was applied unevenly and dripped in many locations. This was likely do to a rushed application process which resulted in uneven layers and was accentuated by the fact that it was applied at an improper ambient temperature.



Figure 13: The new paint job was peeling along the guide bars before the trashracks entered the water. This was likely caused by the fabricators stacking the trashracks before the paint was fully cured.

4.2 Static Structural Analysis

The strength of the structural members on the trashracks was calculated based on the original design of five feet of hydrostatic head. These calculations were performed for the rackbars and the horizontal C15x33.9 beams using basic mechanics of materials equations. Differential head and length, spacing, thickness, and width of the structural members were the driving parameters used to determine the bending and shear stresses in the steel rackbars. The specific parameters were updated for the top and bottom C15x33.9 horizontal beams, but the stress calculations followed the same methodology. A complete list of the static structural calculations is included in Appendix C.1. The critical results are summarized in Table 2.

Table 2: Static structural calculations summary.

Structural member	Head (ft)	Shear stress (ksi)	Bending Stress (ksi)
Rackbars	5	0.2	2.0
Top beam, C15x33.9	5	0.9	10.5
Middle beam, C15x33.9	5	1.3	16.1

All of the static structural stress levels are less than 18 ksi, which is the District's accepted operating limit for A30 steel based on 60% of the yield strength.¹² The bending stress in the middle channel is the only member which is close to 18 ksi. In fact, the shear stress for all members and the bending stress of the rackbar in the direction of the flow are experiencing insignificant stresses. The conclusion can thus be drawn that the existing trashracks are adequately designed for five feet of statically applied differential head.

General hand calculations provided a starting point for the analysis of the trashrack structure, but a finite element analysis (FEA) model was necessary to more accurately grasp the complexity of the geometry. ANSYS Workbench, version 13, was used for a static structural and modal FEA analysis of the trashracks. Figure 14 displays the general Von Mises stress of the trashrack when loaded with five feet of static differential head.

¹² (American Institute of Steel Construction, 1991)

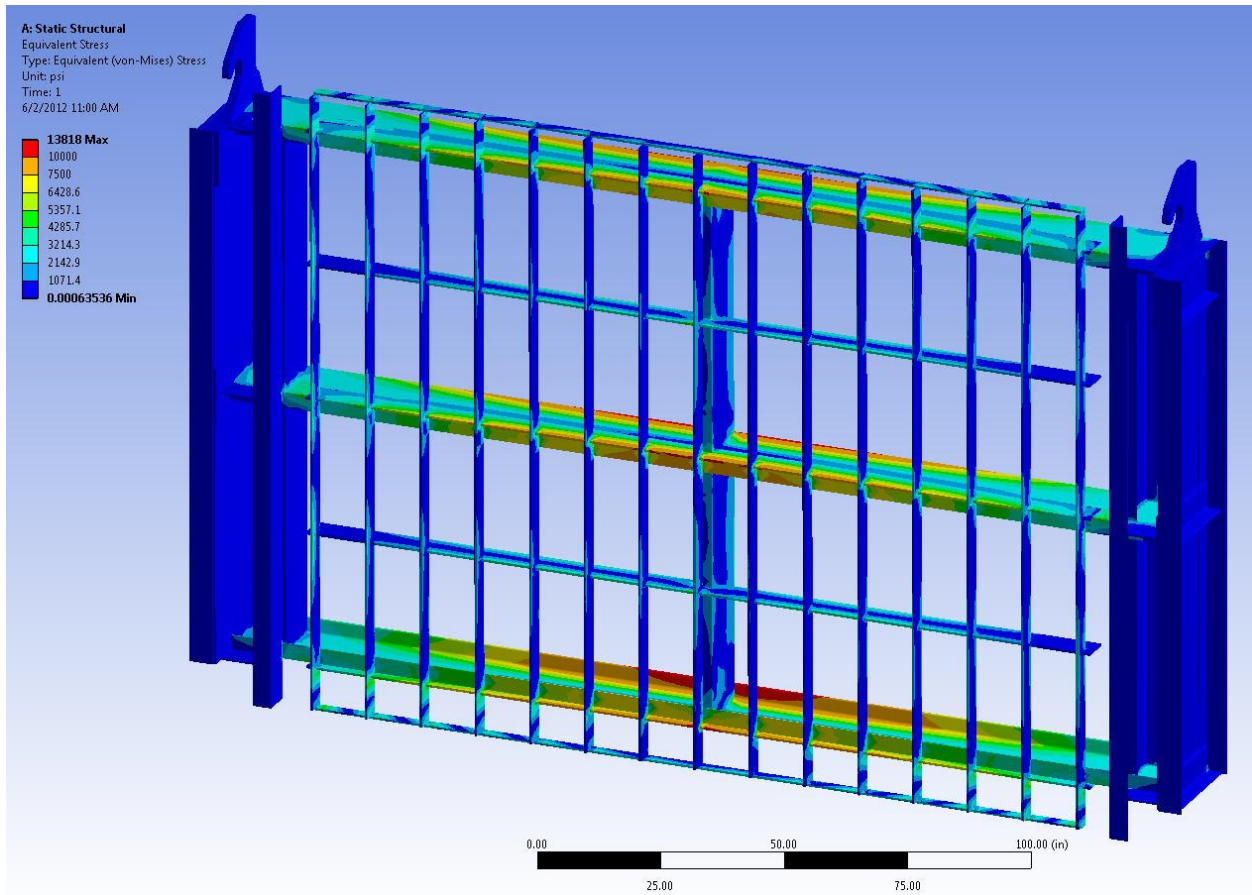


Figure 14: Front view of the trashrack modeled in ANSYS with a static head of 5 ft. The maximum Von Mises stress is 13.8 ksi.

The maximum stress on the trashrack according to the ANSYS results is 13.8 ksi. This occurs along the horizontal beam and is about 15 percent less than the structural hand calculations. A lower stress value from the finite element model is realistic because the model accounts for the distribution of load to the surrounding frame while the hand calculations were for a single beam in bending. Overall, the results of the model and the structural calculations are in close agreement with each other.

A convergence plot for the stress and deformation is presented in Figure 15. This validates the accuracy of the ANSYS solution at the designated mesh. Additional pictorial representations of the model results are provided in Appendix C.5.

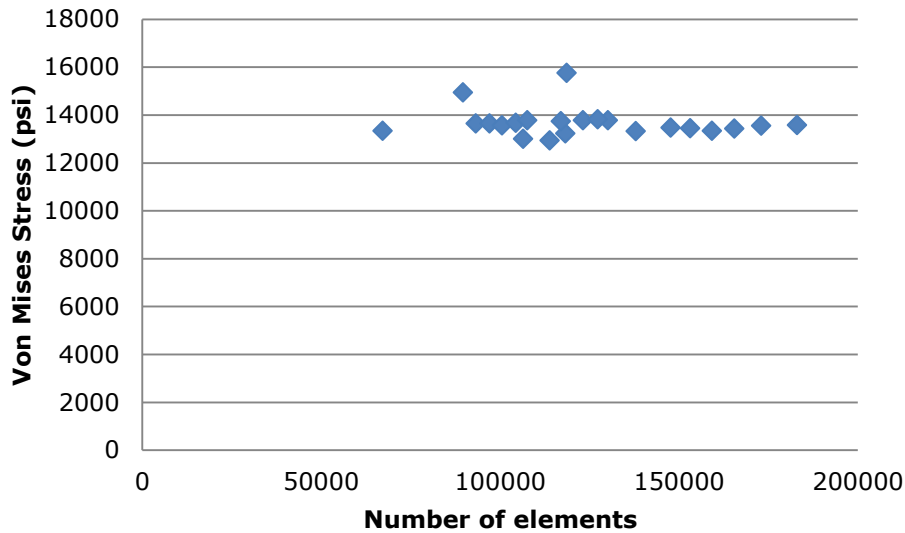


Figure 15: Convergence plot for the maximum Von Mises stress on the trashrack finite element model.

The vibration characteristics of the trashracks were also explored using the finite element model. Refer to Chapter 5 for the extended application of the computer model.

4.3 Fatigue Analysis

The fatigue analysis was conducted according to the stress-life method presented in Shigley’s *Mechanical Engineering Design* textbook. This process is derived from experimental testing from a high-speed rotating-beam machine. An ordinary fatigue strength plot, also known as an S-N diagram, is the basis of this analysis and highlights the endurance limit for steels. From this test, the endurance strength for infinite life is accepted as one half the ultimate tensile strength.¹³

Though the endurance limit of laboratory specimens may be calculated based on experimental results, it is unrealistic for all structural members to adhere exactly to this behavior. Shigley presents Marin’s concept of adding modifying factors to the endurance limit as a way to better represent the material, manufacturing methods, environment, and overall design when conducting a fatigue analysis. Accordingly, the Marin equation may be expressed by Equation 4.1 and the parameters are presented in Table 3.¹⁴

¹³ (Shigley)

¹⁴ (Marin, 1962)

$$S_e = k_a k_b k_c k_d k_e k_f S_e' \quad [4.1]$$

Table 3: Parameters for Marin’s fatigue endurance limit equation.

Parameter	Description
k_a	surface condition modification factor
k_b	size modification factor
k_c	load modification factor
k_d	temperature modification factor
k_e	reliability factor
k_f	miscellaneous-effects modification factor
S_e'	rotary-beam test specimen endurance limit
S_e	endurance limit at the critical location of a machine part in the geometry and condition in use

The Marin equation was used to calculate the fatigue strength for the middle structural beam on the trashrack. This is the beam with the highest stress, as determined by the static structural calculations presented in Table 2. The fatigue strength for the rackbars was not calculated because the operating stress is very low.

Of the modifying factors listed in Marin’s equation, the surface condition and size condition are the only significant terms for defining the proper endurance limit. Structural channels are hot rolled which results in a factor of 0.894. Due to the size and shape of the channel, an effective diameter was calculated which resulted in a size modification factor of 0.70. The loading factor, temperature factor, reliability factor, and miscellaneous-effects factor are all valued at unity because the beam is loaded in bending, the temperature is below 65 degrees Fahrenheit, there is no manufacturing reliability data available, and no miscellaneous items were added.

According to the modifying factors and the rotating-beam endurance limit, the fatigue strength for the A30 steel channel is rated at 17.1 ksi. Complete calculations are provided in Appendix C.2. This is slightly above the maximum stress exhibited at five feet of head.

In addition to calculating a specific fatigue stress operating limit, it is important to realize that fatigue cracks result from the welding defects. Fatigue striations propagate from the defects toward the surface of the trashrack as cracks due to the oscillating nature of the

vibrations. It is unknown where these cracks will occur, and furthermore, they are not discernible by a critical operating stress. Rather, each welding defect, and corresponding crack, will develop at a unique rate according to the size and loading condition. This will also be discussed in the Welding Analysis Section (4.6).

4.4 Vibration Analysis

Fluid induced vibrations on the rackbars were examined based on the calculation of the natural frequency and the forcing frequency. An operating factor of safety was determined based on the ratio of these two vibration frequencies.^{15,16}

The natural frequency calculation for a flat bar of rectangular cross-section perpendicular to its long side within a fluid is given by Equation 4.2. The parameters of the equation are presented in Table 4.

$$f_n = \frac{Kr}{L^2} \sqrt{\frac{gE}{W_b + 0.7W_f \frac{b}{t}}} \quad [4.2]$$

Table 4: Parameters of Levin's rackbar natural frequency equation.

Parameter	Description
f_n	natural frequency
K	coefficient for end fixing of bar; 1.57 for first natural frequency of bar with pinned ends; 3.56 for first natural frequency of bar with fixed ends (existing situation)
r	radius of gyration of the bar about an axis parallel to long side, = $t/\sqrt{12}$ (inches)
t	length of side of bar perpendicular to flow (inches)
b	length of side of bar parallel to flow (inches)
L	span of bar between supports; for bars with half notched ends, effective span is 1.07 times the actual span
W_b	specific weight of bar material (pounds per cubic inches)
W_f	specific weight of fluid (pounds per cubic inches)
g	acceleration due to gravity (inches per second squared)
E	Young's modulus of bar material (pounds per square inch)

¹⁵ (Fortey & Tiry, May 1972)

¹⁶ (Levin, 1967)

The forcing frequency due to vortex shedding of the flat bar is given by Equation 4.3 and the parameters of the equation are listed in Table 5.

$$\text{Forcing frequency: } f_f = \frac{VS}{t} \quad [4.3]$$

Table 5: Parameters of Strouhal's forcing frequency equation.

Parameter	Description
f_f	Forcing frequency
V	velocity of flow past the bar (inches per second)
S	Strouhal number; approximately 0.2, or = $0.12 + 0.012(b/t)$
t	Rackbar thickness

It is recommended that the forcing frequency remain under 40 percent of the natural frequency. Accordingly, the factor of safety between the natural frequency and forcing frequency should be 2.5.

$$\text{Factor of safety: } F.S. = \frac{f_n}{f_f} \quad [4.4]$$

Parameters for the vibration calculations are dependent on the flow rate through the turbine. The typical operating flow rate is currently 7,800 cubic feet per second (cfs), but 9,000 cfs was also calculated as the maximum operating condition. This is the recognized as the runaway condition.

There are three intake bays per turbine in Powerhouse 1, but the flow is not divided equally between the three bays. According to acoustic flow measurements performed on unit B6, 39% of the flow enters through the north intake bay.¹⁷ Though six trashracks are stacked within each bay, it is assumed that 90% of the flow passes through the three bottom steel racks. From this assumption, the final flow rate through each trashrack was calculated to be 3,159 cfs.

An additional flow consideration was the size of the concrete opening leading up to the dam. Units 5 and 6, in comparison to units 7 through 10, have less intake area because of an

¹⁷ (Cartier, Lemon, Greenway, Vuong, & Boubnov, 2000)

extended concrete breast wall. The calculated intake area for units 5 and 6 was 396 square feet and the calculated intake area for units 7 and 10 was 450 square feet.

A complete list of the vibration calculations is included in Appendix C.3. Table 6 presents a summary of the results from the 7,800 and 9,000 cfs calculations. The table is significant because it identifies a natural frequency of approximately 85 Hz and an operating frequency between 30 and 40 Hz for the rackbars. A factor of safety below 2.5 is observed for the higher flow rate which is not ideal, but does not outline a clear failure either. Rather, it simply suggests that the forcing frequency and the natural frequency are questionably close.

Table 6: Vibration calculations summary.

Description	Summary of Calculations			
	5 & 6		7 to 10	
Unit	7,800	9,000	7,800	9,000
Flow rate into turbine (cfs)	7,800	9,000	7,800	9,000
Natural frequency (Hz)	84.5	84.5	84.5	84.5
Forcing frequency (Hz)	35.8	41.3	31.5	36.4
Factor of safety	2.4	2.0	2.7	2.3

The factor of safety against resonance identified in this section is not ideal, but it is not alarming enough to justify the need to completely replace the trashracks. As will be discussed in the Section 4.9, Rehabilitation Recommendations, it is expected that the rackbars would have failed by now if vibrations were a concern. Thus, the existing design is adequate. Chapter 5 will revisit the results from Table 6 while also drawing from the physical test data and the finite element model results.

4.5 Corrosion Analysis

Corrosion damage was visibly alarming across the all of the trashracks when they were removed from the water. Fortunately, the ensuing physical examination determined that no failures, excluding the tie rods, were caused by corrosion. That said, the corrosion damage was still a major concern because of the unknown effect it has on applied factors of safety. Information on the damage was gathered by taking pictures, recording notes, and removing corrosion deposits with a hammer, a steel brush, and a cloth rag. This section will discuss the discoveries of the corrosion investigation and analyze the significance of the corrosion mechanisms exhibited across the trashracks.

The trashracks were originally coated with coal tar epoxy. This was a very common form of corrosion protection for marine environments which reached a peak of popularity in the 1960s. It is an inexpensive and tough coating consisting of a mixture of tar and epoxy. Exceptional elasticity and hydrophobic properties made it an ideal choice for the original protection of the steel trashracks. In essence, coal tar epoxy is very good industrial paint. An orange finish coating is apparent on the structure. Presumably, this final coating was applied to prevent tar from oozing off the racks and into the water. As a side note, coal tar epoxy was essentially decommissioned in the 1990s because of the toxicity of tar.¹⁸ Due to the lack of maintenance records, it is unknown how long the protective coating remained effective. What is known is that corrosion is obvious across the trashrack.

Corrosion is evident by the tubercles on the trashrack. These growths, which have a similar appearance to barnacles, are rust deposits. They are hard to the touch, but can be easily removed with simple tools, such as a hammer and a steel brush. Figure 16 displays some individual tubercles and Figure 17 displays how the tubercles have spread to attack an entire surface.



Figure 16: A grouping of individual tubercles.

¹⁸ (Oman)



Figure 17: Widespread growth of tubercles.

The rough surface appearance is bad, but the situation becomes ugly when these corrosion deposits are removed. Figure 18 and Figure 19 show what lies beneath the surface of Figure 16 and Figure 17.



Figure 18: Corrosion damage under a few individual tubercles.



Figure 19: Corrosion damage under a surface covered with tubercles.

Extreme pitting is evident beneath the tubercles. Pitting is extremely destructive to the strength of the structure because it is a localized attack. The material losses are not uniform, and create stress concentrations across the steel structural members. The most alarming corrosion damage occurs at the welds. Stress concentrations naturally exist at the welds, and the influence of corrosion emphasizes this effect. Figure 20 displays corrosion deposits at a welded joint and Figure 21 shows what remains after some of this debris has been removed.



Figure 20: Corrosion deposits along a welded joint.

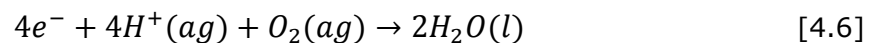


Figure 21: Corrosion damage after the tubercles have been removed from the weld.

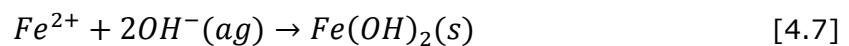
The general reactions in pitting are the dissolution of metal and the reduction of oxygen. Specifically, this results in the formation of $Fe(OH)_3$, Fe_3O_4 , Fe_2O_3 , and other oxides. Chemical equations are provided in the next few lines to outline the process through which this rust forms. It begins when water in contact with the steel causes the droplets to oxidize.



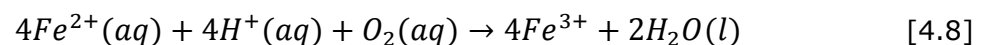
Electrons are picked up by the hydrogen ions and dissolved oxygen which produces water.



As the electrons consume hydrogen ions, hydroxide ions are produced which reacts with the iron to produce iron(II) hydroxides.



Iron(II) ions also produce iron(III) ions when reacting with hydrogen ions and oxygen.



Iron(III) then reacts with hydroxide ions to produce iron(III) hydroxides.



As shown by these reactions, hydrated iron oxides are the most common corrosion products. From these products, Fe_2O_3 is produced, which are the common tubercles, and Fe_3O_4 is produced, which forms under low oxygen concentrations.¹⁹ The iron products are deposited around the pits and create an oxygen concentration cell at each location. A self-stimulating and self-propagating system then encourages rapid dissolution within the pit. An excess of positive charge is developed in the area, which attracts harmful ions, such as chloride ions, to the pit. The presence of concentrated hydrogen and chloride accelerate the corrosion which is why the pitting process is known to be autocatalytic.²⁰

As mentioned earlier, the trashracks were initially fabricated with a protective layer of coal tar epoxy. This was probably a great way to protect the structure, but neglect led to the current corrosion issues. Coal tar epoxy should perform well for about 15 years before it must be reapplied. No maintenance has been performed in the past 11 years, and maintenance records are not available prior to 2000. Under the assumption that no maintenance was performed over the 60 year lifespan, it is not surprising to see such widespread corrosion damage.²¹

Corrosion likely first attacked the steel structure through holidays in the coal tar epoxy. Holidays could have formed as the structure deformed from the flow of the river or by abrasives in the water. The Columbia River is a fresh water river but does contain natural particles. The steel trashracks are stacked from the bottom of the riverbed up about 35 feet which exposes them to sand and other debris suspended in the water.

Erosion corrosion is evident on the surface of the rackbars facing the flow of the river. This can be observed in Figure 22. Minimal protective coating remains on this leading surface and the material is visibly impaired. Abrasives in the water were likely the first mechanism to penetrate the coating which would have initiated the corrosion. Once initiated, erosion corrosion would have continued to accelerate the corrosion by creating more holidays for

¹⁹ (Roberge)

²⁰ (Fontana, 1976)

²¹ (Corrosion Control Products Company)

pits to form. Furthermore, the anodic areas where pits formed from the holidays would be small in area compared to the protected cathodic region which initiates the unfavorable area effect.²²



Figure 22: Erosion corrosion damage of leading edge.

Erosion corrosion rates are typically tied to a critical flow velocity. Corrosion rates rise significantly at this critical flow velocity, similar to a ductile to brittle transition temperature. Though the critical flow velocity is not known for this environment, it can be assumed that the velocity is above this limit because of the sullied surface.

Velocity effects manifest themselves in other ways too. Fresh water corrosion systems are not usually affected by hydrogen evolution because the pH is too high. In this situation, the flow of water either increases corrosion by bringing oxygen to the steel or by developing partial passivity by supplying excessive oxygen. Figure 23 displays the corrosion rate versus velocity for rough and polished steel.²³ The operating flow velocity on the trashracks under investigation is typically four to six feet per second, which places the corrosion rate in the passive zone, regardless of the surface finish. From Figure 23, it can be concluded that the velocity effect due to oxygen reaching the surface is not critical to the corrosion failure. This means that the mechanical erosion rate is the more significant problem.

²² (Natesan, 1980)

²³ (Revie & Uhlig, 2008)

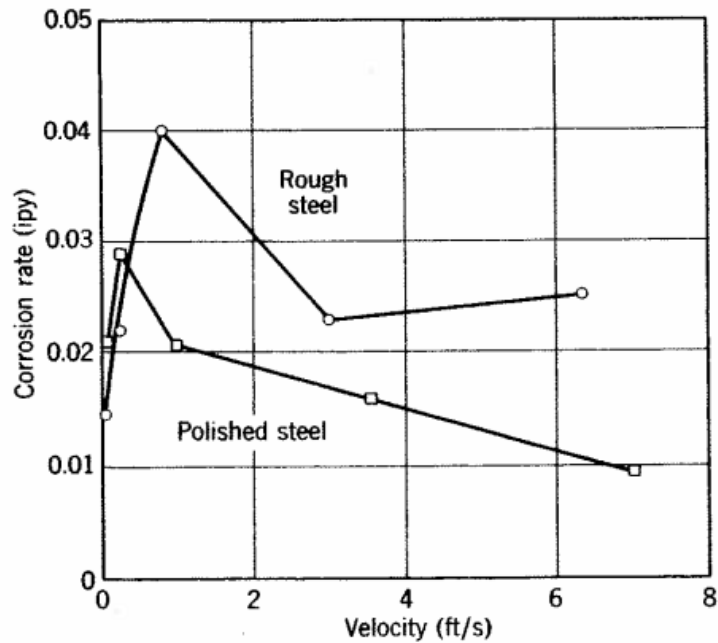


Figure 23: Corrosion rate versus velocity for steel in fresh water.

The sections above were laid out to postulate that holidays in the coal tar epoxy, likely caused by erosion corrosion, allowed pits to form under the paint which became oxygen concentration cells. In addition to the corrosion analysis on the pits, the effects of biologically influenced corrosion were also examined. Biological deterioration of metals, commonly known as microbiologically influenced corrosion (MIC), is a harmful mechanism that was likely present on the trashracks.

Biological corrosion begins with the formation of a biofilm consisting of a living biological mass. Bacteria, algae, and other microorganisms present in the biofilm can produce metal dissolving products, such as sulfuric acid.²⁴ These living organisms are sustained by chemical reactions in which they inject reactants and eliminate waste. Some of the adverse effects observed by these processes include influencing the anodic and cathodic reactions, influencing the protective film, and producing deposits.²⁵ An attack on the protective film and the consequent production of deposits were the most significant issues for the trashracks. As observed in Figure 24, biological growth does exist on the structure. Though it was technically unknown whether these organisms were toxic and created holidays in the

²⁴ (CorroView International)

²⁵ (Fontana, 1976)

paint, the issue of MIC was eventually dismissed as a critical concern. The growths were easily removed and did not show visible signs of penetration through the paint.



Figure 24: Example of biological growth.

Galvanic corrosion around the bronze springs on the trashrack was another corrosion problem. Steel is anodic to bronze according to the galvanic charts. The galvanic coupling effect is a problem for the bolts which secure the bronze springs to the trashrack. Original drawings specify to hot galvanize the steel bolts, nuts, and washers. Unfortunately, this coating is sacrificial in nature and likely wore off decades ago. Figure 25 displays the corrosion deposits at the top of the bolts. Corrosion is visibly evident on the top of the bolt, but the cross section of the shank was not noticeably reduced. Considering that the loss of material was not obvious on the bolt after 60 years, it was concluded that galvanic corrosion of the bolts was not a concern.



Figure 25: Galvanic corrosion due to coupling of steel bolt to the bronze spring.

Although deterioration is evident from pitting and galvanic action, fretting corrosion at the tie rods was the only complete corrosion failure identified during the field inspections. The 7/8 inch diagonal tie rods were falling out of the trashrack during normal operations, and part of the reason was extreme fretting corrosion. Fretting corrosion is defined as damage occurring at the interface of two contacting surfaces. It occurs in the presence of mechanical stresses and commonly includes vibrating members. The mechanism is part chemical and part mechanical. Mechanically, the contacting surfaces, known as asperities, rub off protective layers to expose fresh metal. Chemically, this exposed layer of metal is readily attacked by corrosive environments.²⁶

The diagonal tie rods are known to vibrate excessively in the flow of the water. These rods are attached through the structural channel members, but the connection appears to wear out after years of use. Figure 26 shows the end of a significantly compromised tie rod that has been removed from the rack. The direction of material deterioration is quite evident from the picture. A rather smooth surface remains where the mechanical wear attacked the rod. Surrounding areas have a much rougher surface texture which proves corrosion was attacking the surface.²⁷ The progressive nature of fretting corrosion was one of the main reasons that the Rehabilitation Recommendation section states that the existing tie rods should be removed and replaced with a welded brace.

²⁶ (Revie & Uhlig, 2008)

²⁷ (Revie & Uhlig, 2008)



Figure 26: Fretting corrosion evident on the steel tie rod.

Between the pitting corrosion, erosion corrosion, biological corrosion, galvanic corrosion, and fretting corrosion, it was concluded that the pitting damage beneath the tubercles was the most destructive corrosion mechanism on the trashracks. A maximum pit depth of 0.12 inches was measured during the inspection. Based on 60 years of service, this indicates a corrosion rate of two milli-inches per year (mpy). The observed corrosion rate was even within the commonly acceptable range of five mpy if it is assumed that the coal tar epoxy completely protected the steel for 35 years.

Though the corrosion rate was likely below the critical rate of five mpy, the pits do create stress concentrations on the trashracks. The stress concentrations are of greatest concern around the welds where the stresses are highest because the joints are fixed. Considering the amount of corrosion damage which developed over the 60-year lifespan of the trashracks, it is quite impressive that pits near the welds did not lead to stress overload failures in the structural members or vibration runaway failures on the rackbars. It seems as though the coal tar epoxy deserves significant credit for effectively protecting the steel for many years. However, the current lack of failures due to corrosion became a solid justification that the structure was acceptable for continued operations in the current state. The one caution is that it is mandatory that the trashracks need to be protected against future corrosion damage. Recommendations outlining the protection methods are provided at the end of this chapter.

4.6 *Weld Analysis*

The weld analysis began by verifying that the size of the existing welds was sufficient to support the required hydrostatic load. Blodgett's *Design of Weldments* provided the model

for analyzing the welds.²⁸ This set of calculations determined that the most critical welds have a factor of safety of at least 3.5 based on a very conservative approach. Refer to Appendix C.4 for the specific calculations.

Though the original welds were adequately sized, it was eventually discovered that many of the welds had inclusions or undercut defects. Nearly all of the defects were identified on the welds connecting the rackbars to the trashrack structure. The welds joining the structural channels appear to have been constructed without noticeable inclusions or undercut. Refer to the Field Inspection Section (4.1) for the discussion about the discovery of these welding defects.

The existence of welds with undercut and inclusions identified a major source of stress concentrations within the welds. These stress concentrations significantly decrease the factor of safety of the rackbars due to vortex shedding. The unknown aspect is how far below 2.0 the safety factor falls. Based on the Weld Analysis and the Field Inspection, it is safe to conclude that the welds on the structural members are sufficient for continued operation, but the cracked welds attaching the rackbars need to be replaced to avoid complete fractures. Welds around the rackbars without cracked welds do not need to be replaced because it can be assumed that any critical stress concentrations would have led to cracks after 60 years of operation.

Deciding to replace cracked welds but leave non-cracked welds was not a trivial decision. Vibrations of the rackbars create a fatigue concern which amplifies any defect in the welds. There could be many cracks which have not propagated to the surface yet and others not identified by the MT tests. However, an economical decision had to be made which in this case resulted in the replacement of only cracked rackbars.

4.7 Design of Diagonal Braces (Tie Rod Replacements)

The original trashrack design specified that four 7/8 inch rods extend diagonally from the center of the rack to each of the four corners. These diagonal tie rods ensured that the trashrack structure was rectangular prior to deployment in the trashrack slot and also provided lateral stability while handling the racks with the gantry crane. The cross sectional area of the rod was adequately sized to support the desired structural loads. Unfortunately,

²⁸ (Blodgett, 1966)

it was not properly selected to combat the vibrations due to vortex shedding. More than half of the tie rods were missing during the field inspection and the remaining rods were noticeably loose. This was a clear justification that the tie rods needed to be replaced. The selection process for the new tie rods was guided by two constraints; the new rods must be at least as strong as the existing design and the geometry must be selected to decrease vibrations. One of the first decisions made was to specify that the new tie rods be welded in place rather than use a bolted connection. The original tie rods extended through the structural channels and were secured by bolts on the ends of the threaded rods. Properly welded joints combat vibration concerns much better than the original threaded rods. All structural validations of the tie rods were completed through static deformation tests in ANSYS. Optimization for fluid flow was based on Strouhal number characteristics compared to the stability of the section modulus.

The finite element model in ANSYS was first used to establish guidelines for the placement and orientation of the tie rods. Five points are presented below as determined by the analysis. At this point, the reader will notice the transition to referring to the tie rods as braces. This is due to the forthcoming decision to use a structural component rather than a rod for the diagonal support member.

1. Two structural steel components (channels, angles, and larger rods) provide twice as much stiffness as the original four 7/8 inch tie rods. Therefore, only two braces are required.
2. Braces positioned in the top half of the trashrack are slightly stiffer than braces positioned in the bottom half of the trashrack. Therefore, the two braces will be located in the top half of the trashrack.
3. Braces oriented in the same direction as the original tie rods are stiffer than braces extending from the opposite corners of each quadrant. Therefore, the two braces will follow the existing direction of the tie rods.
4. Braces attaching at the junction of the horizontal and vertical channels decrease the induced moment as the trashracks deform. Therefore, the two braces will be connected to the structural members directly through the center of each corner connection to prevent the development of stress risers.
5. A comparison between angle irons, channels, and rods of varying cross sections determined that the cross sectional area is the driving factor in strength and that geometry does not factor into the determination of diagonal stability. Therefore, as

long as the cross section was above 0.6 square inches, the brace with the best flow characteristics could be selected.

This initial round of structural requirements narrowed the possible braces to a rod with a diameter of at least 1.25 inches, an angle iron of size L2x2x0.375, or a channel of size C3x4.1. An L2x2x0.25 also met the minimum structural criteria but was not selected because the thinner legs of the angle would be much more susceptible to corrosion damage. Hollow structural steel (HSS) was not explored because corrosion damage would progress rapidly if water reached the inside of the tube. The drag force on each of these three members is well within an allowable limit. Table 7 presents the drag force and corresponding shear and bending stresses on the rod and angle according to Equations 4.10 and 4.11. The angle iron was rotated 45 degrees into the flow, such that the elbow of the angle was pointing directly toward the flow. Rotation of the angle was determined by the preferential optimization of low drag in the direction of flow and high stiffness perpendicular to the flow. The channel is not included in the table because it did not have any strength or vibration advantages over the angle. A complete set of the calculations is provided in Appendix C.6.

$$F_D = \frac{1}{2} C_D A_p \rho V^2 \quad [4.10]$$

$$\sigma = \frac{Mc}{I} \quad [4.11]$$

Table 7: Coefficient of drag, drag force, shear stress, and bending force for the original rod, the potential 1.25" rod and the potential two inch angle.

Description	Variable	Units	Original 0.875" Rod	1.25" Rod	L2x2x0.375
Coefficient of Drag	C_D	-	1.17	1.17	1.55
Drag force	F_D	lbf	7.3	10.4	30.8
Shear stress	V	psi	6.0	4.2	11.3
Bending stress	σ	psi	1498	734	1806

Vibration characteristics of the braces were explored after establishing the initial structural equivalency requirements. The fluid induced Strouhal forcing frequency and the structural section modulus were used to compare the rod and the angle. Table 8 and Table 9 present

the comparisons of these vortex shedding frequencies and section modulus values. The forcing frequency calculations were performed according to Equation 4.3.

Table 8: Vortex shedding frequency according to the Strouhal number.

Description	Variable	Units	Original 0.875" Rod	1.25" Rod	L2x2x0.375
Strouhal number	-	-	0.2	0.2	0.175
Vortex shedding frequency	f	Hz	21.9	15.3	6.0

Table 9: Comparison of section modulus values for the rods and the angle iron braces.

Section Modulus	Original 0.875" Rod	1.25" Rod	L2x2x0.375
Direction of flow	0.066	0.191	0.229
Perpendicular to flow	0.066	0.191	0.532

Before presenting the final replacement for the 7/8 inch tie rods, it is important to discuss the option of no tie rods. Removing the tie rods, and not putting diagonal supports back in, is the preferred engineering solution. Lateral stability is not required while the unit is operating, and removing the tie rods reduces the flow losses while also simplifying the number of structural liabilities on the trashracks. However, the tie rods are an important safety feature while moving the racks with the gantry cranes. "Single picking" of the trashracks, when the gantry crane only lifts one side of the rack and wedges it in the trashrack slot while plastically deforming the structure, is a realistic concern because it happened with a head gate just a couple of years ago. Accordingly, it was recommended that braces be installed, though the complete removal of the tie rods would decrease the required fabrication, decrease the rehabilitation costs, and decrease the impact on the flow.

Based on the data presented throughout this section, the L2x2x0.375 angle iron was selected as the diagonal brace on the trashracks. This selection may appear a bit odd because the vortex shedding frequency of the angle iron is less than half the frequency for the 1.25 inch rod. That is significant because it indicates that vibrations will not be initiated as easily on the rod. However, it is critical to note that the section modulus of the angle is more than double that for the rod. In addition to decreasing the deflection of the induced vibrations, this also significantly increases the natural frequency of the angle compared to the rod. Thus, though the angle has a lower forcing frequency, the spread between the natural frequency and the forcing frequency is greater, which is the most critical fluid dynamic comparison.

4.8 Rehabilitation Recommendations

The Rehabilitation Recommendations section highlights the list of action items submitted to the District in November 2011. The field inspections, structural analyses, and vibration calculations had been completed at this time. The calculations and FEA model validated that the general trashrack design, with the exception of the tie rods, was adequate to last another 40 years.

This is a unique section in chapter four because it is effectively the conclusion to the failure analysis project. The action items included below were carried out on the trashracks between November 2011 and February 2012. Each of the items in this section are printed as they were originally presented to the District. Though the Rehabilitations Recommendations section is slightly different than the rest of the report, it is included to demonstrate that the analysis led to a set of specific design decisions which were executed by Chelan County PUD. The repaired set of trashracks was returned to the operating slots of unit B9 in February 2012.

4.8.1 Remove Tie Rods

The original 7/8 inch tie rods should be removed. Tie rods in high flow conditions, specifically on the steel trashracks, have been found to fracture near the connection to the horizontal channel members. Tie rods in lower flow conditions, specifically on the wood trashracks, have been found to vibrate sufficiently to mechanically wear through the connection point until failure occurs.

4.8.2 Sandblast and Paint

Sandblast the trashracks to near white metal and paint with coal tar epoxy to a thickness of 24 mils. The District's painting specifications for submerged metals are provided in Appendix D.

4.8.3 *Repair Cracked Welds*

Use non-destructive evaluation techniques, per District specifications, to identify indication of fractures within the welds. Completely gouge crack areas and re-weld the affected area, per District specifications.

4.8.4 *Replace Tie Rods*

The four 7/8 inch tie rods should be replaced with two angle iron braces. Two structural braces will provide more stability during a single pick situation than the existing configuration. Furthermore, the recommended configuration was optimized to decrease vibration and drag. Following is a description of the recommendation:

- Install two L2x2x0.375 pieces of angle iron on the top half of the trashracks.
- Follow the existing orientation of the top tie rods.
- Use structural steel, A36.
- Rotate the angle iron 45 degrees, such that the outer edge of the elbow is the leading edge to approaching flow.
- Align the neutral axis of the braces directly with the intersection of the horizontal and vertical structural channels.
- Use full penetration welds during fabrication.
- On the steel tracks, position the elbow of the angle iron so that it butts against the top 6"x0.5" horizontal rackbar. Weld these connecting points together.
- On the wood trashracks, position the angle iron braces at the center of the horizontal structural channel members.

Note: Complete removal of the tie rods, which would decrease the required fabrication, decrease the rehabilitation cost, and decrease the impact on the flow was the favored design decision. This is possible because the tie rods are not necessary when the turbine unit is operating or when the trashracks are lifted by both gantry hooks. However, this option was not recommended because the gantry cranes can be challenging to operate and "picking" a trashrack with one hook is a real possibility. Diagonal braces provide significant stability in the case of a single hook pick.

4.8.5 Replace Wood

Douglas fir wood was ordered from Western Materials to replace the existing wood bumpers and rackbars. 72 wood bumpers should be cut from the 10"x10"x10' ACQ 0.60 treated lumber according to W.H. Reller Drawing 137-5. 135 rackbars should be cut from the 3"x8"x12' ACQ 0.60 treated lumber according to W.H. Reller drawing 137-5. All cut surfaces should be coated with Copper-Green Wood Preservative.

Attach the wood to the steel trashrack frame with galvanized fasteners and bronze wood screws. Refer to W.H. Reller drawing 137-1 for the general assembly configuration. The hardware for this project is located just inside the "C" building in the boneyard. It is a mixture of existing galvanized stock, reusable bronze fasteners, and new hardware from Fasteners. Please note that the #30 wood screws were not available, and thus #24 wood screws will be used as a replacement.

4.8.6 Maintenance Recommendations

Maintenance recommendations were provided to Chelan County PUD along with the rehabilitation recommendations. The scheduled cleaning and inspections were premeditated to avoid unforeseen problems with the trashracks in the future and catch them early if anything damaging begins to occur.

4.8.6.1 Clean the Trashracks

The trashracks should be cleaned on a regular schedule. There is a direct correlation between the accumulation of trash, generating efficiency, and profits for the company. Annual cleaning should be mandatory, though biannual cleaning would be preferred. Scheduling the cleaning early in the summer, following the high river flows and preceding the late summer generating demands, would be a simple way to maintain maximum generating efficiency. The debris should never be allowed to accumulate such that a differential head of more than five feet is observed across the trashracks.

Units B9 and B10 need to be cleaned much more frequently than the other units. These units, located closest to the North spill gate, attract significantly more trash than the other units at Powerhouse 1.

4.8.6.2 *Inspect Rehabilitated Trashracks*

Scheduled inspections should be initiated following the rehabilitation project. The south set of six trashracks from B9 should be inspected within two years of commissioning. All of the B9 trashracks should be inspected within five years of commissioning.

Inspections are necessary to identify fractured members and repair chips in the paint. Impacting debris pierces the tough epoxy coating, exposing the steel to corrosion. If left untreated, water will penetrate the steel under the paint and create a self-perpetuating corrosion cell under the layer of paint. Localized paint repairs should be performed during the inspections to prevent the growth of corrosion. Corrosion damage over the next 40 years is likely to be an issue, but can be prevented. Sacrificial anodes offering cathodic protection should be explored as a potential solution to corrosion prevention if the epoxy paint does not provide the required level of protection. Furthermore, it would be a good idea for the District to test the corrosiveness of the water to characterize the level of attention that should be placed on protecting future systems from corrosion. These tests should be performed at multiples times during the year because the temperatures and chemicals in the river fluctuate by the season.

The need for future inspections should be identified based on the condition of the trashracks after five years.

Chapter 5: Vibration Experiments

5.1 *Vibration Overview*

An extended vibration study was conducted during the project to complement the structural analysis presented in Chapter 4. This dynamic analysis was the most research oriented aspect of the case study. Experimental vibration data was gathered in September 2011 and post-processed in MATLAB. The objective was to determine whether the results from the vibration data, vibration calculations, and finite element model exhibited correlating responses.

Vibration calculations targeting the lateral movement of rackbars on the trashracks were presented in Section 4.4. This analysis followed Levin's implementation of the Timoshenko beam theory based on a modified material density. A natural frequency of 84.5 Hz was identified in Section 4.4 for the 28.5 inch rackbars. Using the same approach, a 57 inch rackbar, essentially two smaller rackbars translating together, has a calculated natural frequency of 21.1 Hz. In reality, the natural frequency of the extended rackbars should be higher than 21.1 Hz because a horizontal stiffener couples the rackbars to the center vertical channel. The calculated Strouhal forcing frequency is velocity dependent and reaches a maximum frequency of 35 Hz at the maximum flow rate. These theoretical calculations provide base level information used for the assessment of, first, the experimental data and, then, the finite element model.

5.2 *Experimental Data*

Experimental data was gathered on September 19 and 20, 2011, at Rock Island Dam. A tri-axial accelerometer and 15 strain gauges were applied to the second trashrack from the bottom in the north intake slot of unit B9. Strain gauges were placed at strategic locations on the trashrack to target vibrations of the rackbars, stress levels near the welds of the rackbars, vibrations of the tie rods, and stress levels in the structural members. The tri-axial accelerometer from PCB Piezotronics IMI Sensors Division was bolted to the center of the middle, horizontal beam on the trashrack. This accelerometer was calibrated at the manufacturing facility with a reported sensitivity of 100 mV/g in the X direction, 99 mV/g in the Y direction and 98 mV/g in the Z direction. The output signal was sent through a PCB Piezotronics signal conditioner with a gain of unity. Data was gathered at a sampling rate of 2,000 samples per second and processed through Vishay Micro-Measurement's 24-bit

System 7000 data acquisition system. The main intent of the experiment was to monitor the physical vibrations during normal operating conditions to provide a baseline dataset to compare to the vibration calculations and vibration model. A secondary goal of the experiment was to determine the maximum stress levels at various locations on the trashrack.

Though data from the strain gauges was recorded during the tests, the accelerometer proved to be the only source of reliable data. An ambient signal of 60 Hz in the water from the power lines at the dam dominated the strain gauge signal and interfered with the data. Fortunately, the accelerometer produced a reliable signal, though the voltage range could have been adjusted to increase the resolution of the output.

Trashrack vibrations are excited by the flow of water through the steel mesh. Vortex shedding tendencies and pulsating drag initiate various modes of vibration on the trashrack. Sweep tests and step tests were used to experimentally explore these vibrations. Sweep tests consisted of recording data while slowly progressing from zero flow through the trashracks to the maximum flow condition. These sweep tests were conducted over the course of about five minutes. For simple vibration studies, sweep tests should be sufficient to excite all mode shapes. However, due to the complexity of the trashrack structure and to ensure that there were no transient responses, step tests were used to validate the results of the sweep tests. Step tests consisted of recording data for 90 seconds once the flow rate had reached a specified steady state condition.

Data from the tri-axial accelerometer was recorded in the direction of flow, the lateral direction, and the vertical direction. A plot of the general vibrations in the three directions is shown in Figure 27. The maximum flow rate is reached around 100 seconds in the figure and is held constant until the end of the test. Between these three directions, the general vibrations in the direction of flow are about three to four times greater than the vibrations in the lateral and vertical directions. Vibrations in the lateral and vertical direction were of roughly the same lower magnitude. In the direction of flow, the vibrations consistently increase until a marked decrease occurs around 75 seconds. The response in the direction of flow rapidly increases again toward the steady state condition. In contrast, the lateral vibrations have a notable increase in vibrations around 75 seconds before settling to a lower value at the steady state condition. The vibrations in the vertical direction are rather uninteresting because they display the least dynamic response.

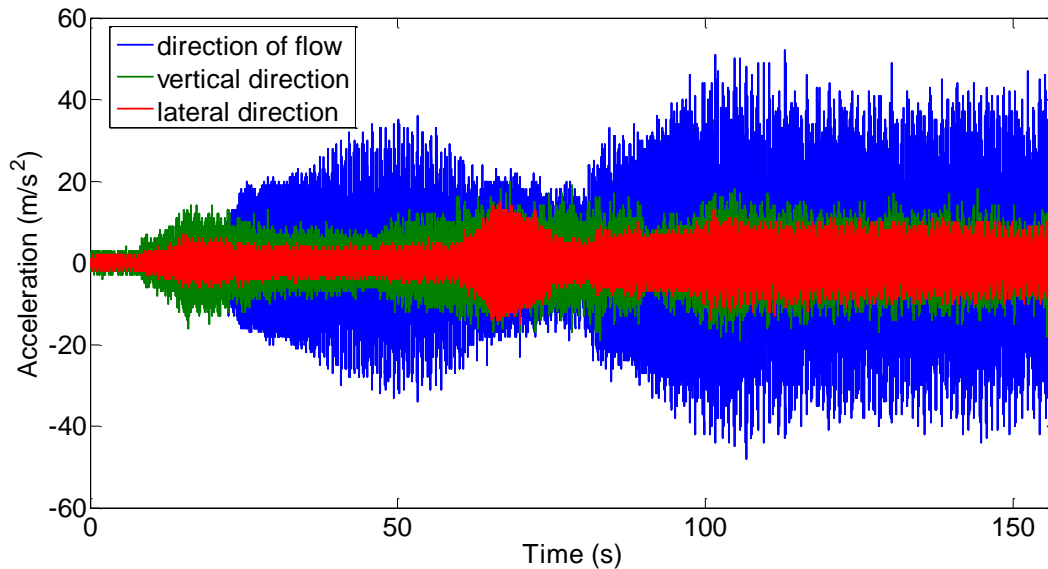


Figure 27: General response of the accelerometer during a sweep in flow rate through the trashrack. Vibrations are plotted in the direction of flow, in the lateral direction, and in the vertical direction.

Acceleration as a function of time provides a general overview of the vibration response but is far from a complete analysis. The remainder of the Experimental Data Section (5.2) explores the frequency response of the system. Vibrations in the direction of flow are the emphasis of the analysis because this response has a much higher magnitude. However, the spike in vibrations in the horizontal transverse direction as the flow approaches the maximum capacity is also explored because of the dramatic increase in magnitude at this flow rate.

Frequency response data was derived from the general response of the accelerometer through the use of a short-time Fourier transform. The short-time Fourier transform was performed in MATLAB through the spectrogram function. This function divides the general response data into consecutive sets of data and performs a discrete Fourier transform on each set. Each set of data is overlapped with the previous set to maintain a high level of resolution in the output. A spectrogram plot illustrates the time-varying frequency data produced by the Fourier transform. Time and frequency are plotted on the X and Y axes while color density represents the magnitude of the response in decibels. Figure 28 is the spectrogram produced in the direction of flow for a sweep in flow rate. The dominant frequencies are shown in the spectrogram plot on the top, while the general response and flow rate data are plotted along the same time axis on the bottom.

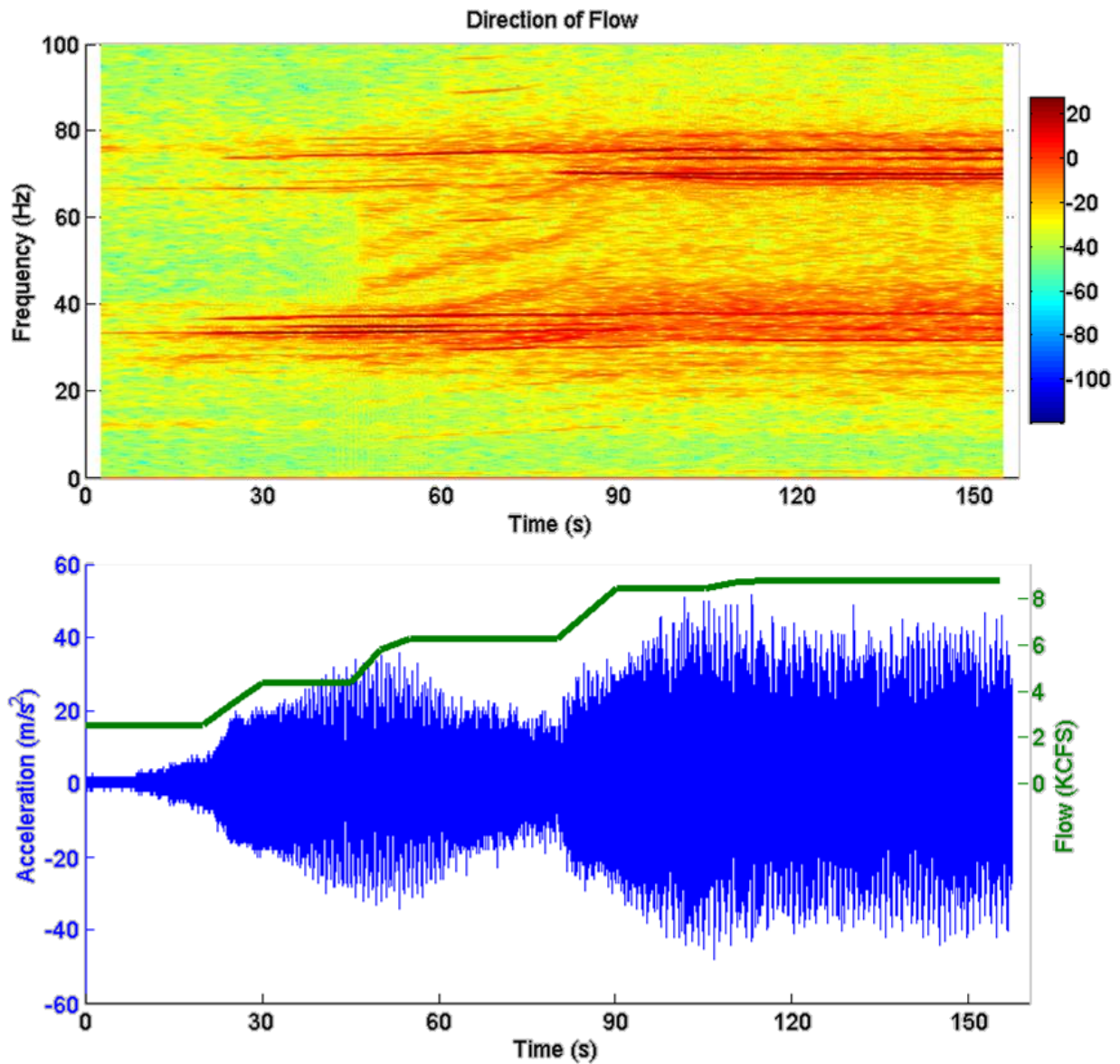


Figure 28: Trashrack vibration response in the direction of flow. The spectrogram plot on the top highlights the dominant frequencies while the bottom plot provides the general response of the accelerometer and the corresponding flow rate. Spectrogram data is presented in decibels and is normalized according to the color bar on the right.

The spectrogram plot shown in Figure 28 presents the data with capped axes. The original frequency range was zero to 1,000 Hz and the time extended for a total of 300 seconds. However, the reduced range was selected because the outlying data did not portray any dominant frequencies and the displacements associated with the vibrations are very low above 100 Hz. A consistent set of axes was used for each of the three accelerometer directions.

Figure 28 is important because it identifies an initially strong response at 35 Hz in the direction of flow which then transitions to 70 Hz at the maximum flow rate. These two frequencies are the natural frequencies of the trashrack because they are independent of the flow rate and the frequency of excitation. Though they are both the dominant frequencies, the magnitude of vibrations at 35 Hz is three times greater than the vibrations in the direction of flow. By the time the maximum flow rate is reached, the response in the mid-30 Hz range decreases to half the magnitude of the 70 Hz response. In addition to the vibrations at the natural frequencies, there are some velocity dependent vibrations which appear at 45 seconds and progress from 35 Hz to 70 Hz for about 40 seconds. Structural damping of the trashrack results in resonance over a range of about 10 Hz around both modes of major vibration. Figure 29 presents the related response in the lateral direction.

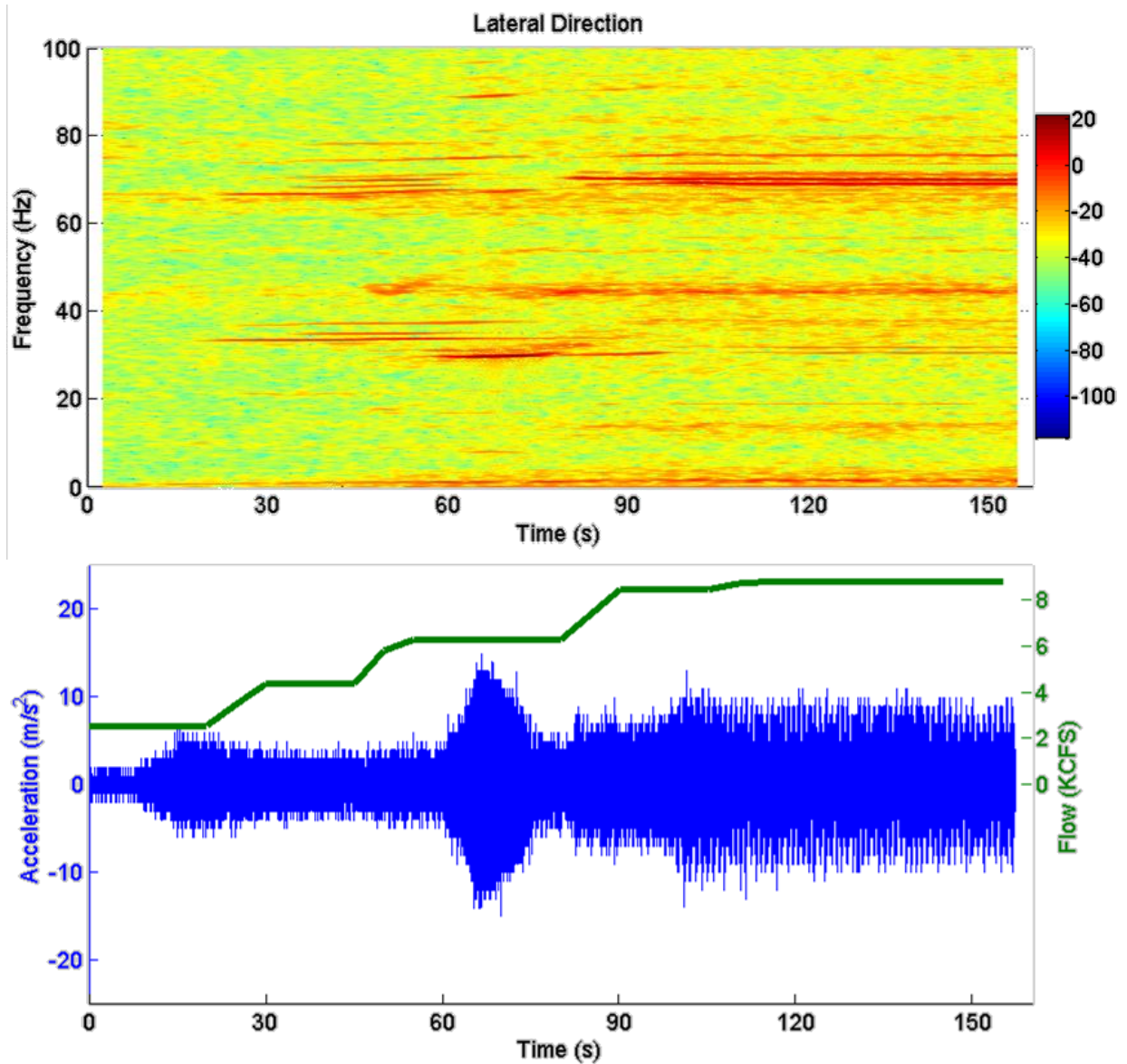


Figure 29: Trashrack vibration response in the lateral direction. The spectrogram plot on the top highlights the dominant frequencies while the bottom plot provides the general response of the accelerometer and the corresponding flow rate. Spectrogram data is presented in decibels and is normalized according to the color bar on the right.

The spectrogram plot for vibrations in the lateral direction, shown in Figure 29, confirms a similar pattern to the vibrations in the direction of flow. There is an initial response in the 30 Hz range that then transitions to 70 Hz as the maximum flow rate is approached. However, the frequencies are much more defined which signifies that the damping in the lateral direction is lower than the damping observed in the direction of flow.

As the flow rate through the trashrack increases, the lateral vibrations first appear at 33 Hz. An extremely dominant frequency of 30 Hz is then observed between 60 seconds and 80 seconds. The higher frequencies of 68 Hz and 70 Hz begin around 80 seconds which is when the flow rate reached approximately 80 percent of the maximum condition. The magnitude of response at 30 Hz is about two orders of magnitude above the maximum flow rate response. It is also roughly half the magnitude of the vibrations in the direction of flow observed in the mid-30 Hz range. The vibrations observed in the lateral direction at the maximum flow rate are also lower than the vibrations in the direction of flow by an order of magnitude. Furthermore, the lateral response at 30 Hz completely disappears by the time the maximum flow rate is reached, which is contrasted by the continued existence of the response in the direction of flow in the mid-30 Hz range regardless of the flow rate.

Figure 30 is the final spectrogram plot and it displays the vibrations in the vertical direction. In comparison to the vibrations in the direction of flow and the lateral direction, this figure portrays minimal resonance. Some vibration resonance can be seen at 30 Hz and 70 Hz, but these vibrations are not nearly as differentiated as the vibrations in the other two directions. Accordingly, the vibrations in the vertical direction are not as critical as the vibrations in the direction of flow and the lateral vibrations.

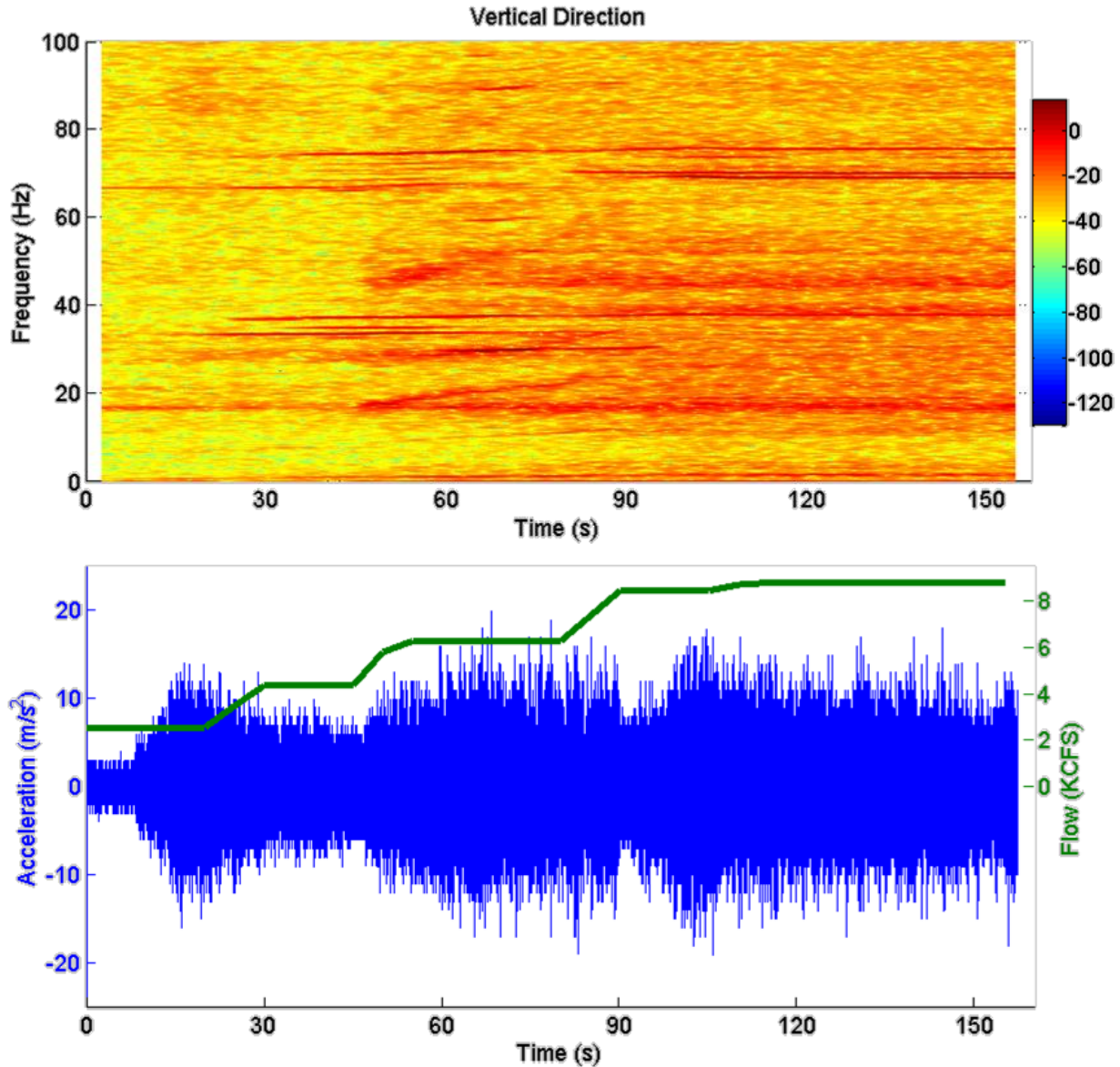


Figure 30: Trashrack vibration response in the vertical direction. The spectrogram plot on the top highlights the dominant frequencies while the bottom plot provides the general response of the accelerometer and the corresponding flow rate. Spectrogram data is presented in decibels and is normalized according to the color bar on the right.

Vibration data from the experimental sweeps is easy to work with because it encompasses all modes of vibration at all operating conditions. However, this method is only accurate if each of the mode shapes is excited from the sweep in flow velocities. Data from steady state flow rates was collected during the experiments to compare to the data represented in the sweep spectrogram. This ensured that the vibration data did not include transient results. Figure 31 illustrates the steady state fast Fourier response plots in the direction of flow at four separate flow rates.

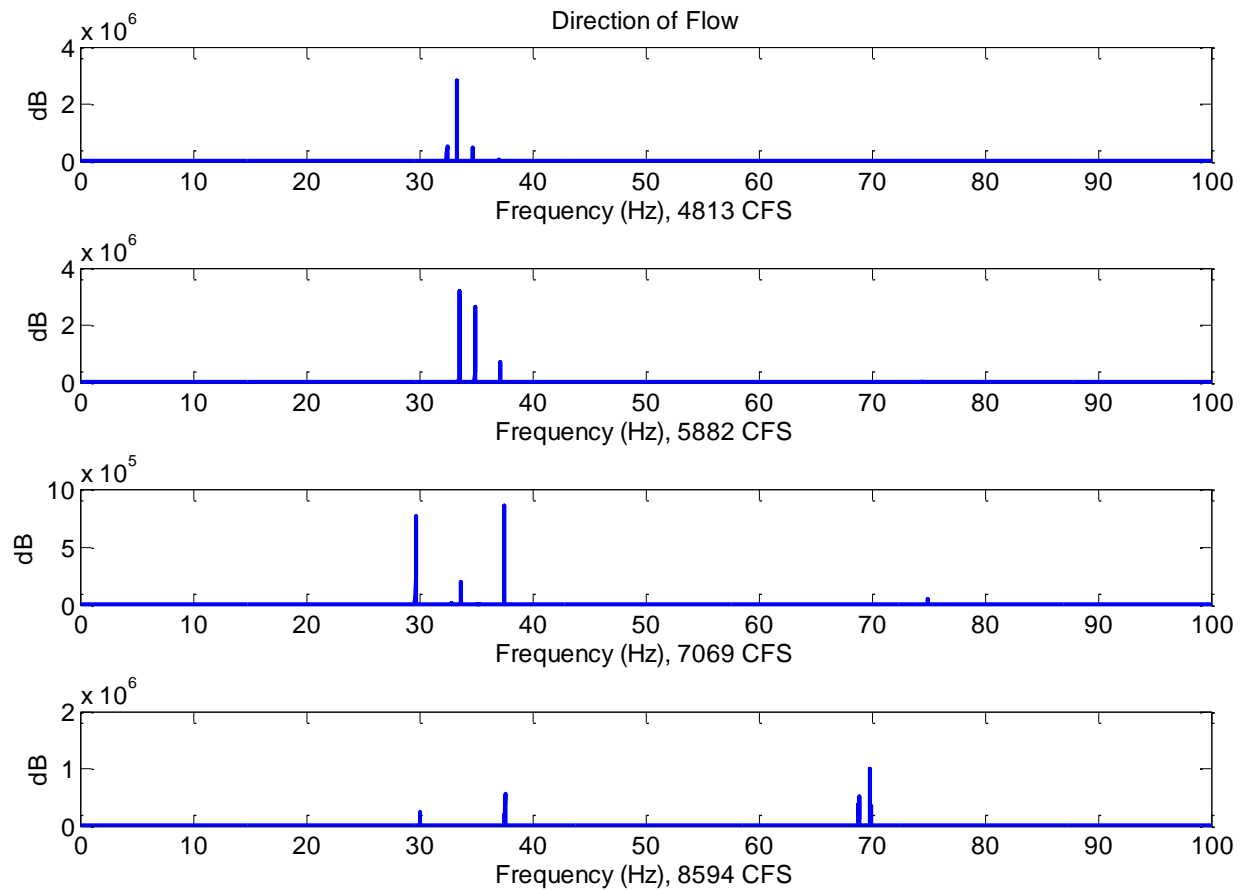


Figure 31: Steady state fast Fourier transform plots at varying flow rates. The power density spectrum for the response data is plotted in units of $(\text{m/s}^2)^2/\text{Hz}$.

The frequencies identified at each of the flow rates in Figure 31 agree with the results from the spectrogram plot. This signifies that the sweep plots did accurately capture the vibration response of the trashrack. Though the spectral power density plots are only provided for the direction of flow, the vibrations in the lateral direction and vertical direction also showed the same positive correlation to their respective spectrogram plots.

The experimental data provided an abundance of information about vibrations on the trashrack, but it does not relate precisely to the vibration calculations. Limited velocity dependent results were observed and there was not a natural frequency at 84.5 Hz. In addition, it is surprising that the response in the direction of flow was significantly greater than the expected lateral vibrations from vortex shedding. The finite element model results presented in the next section provide additional insight.

5.3 Finite Element Model Vibrations

The same finite element model used in Section 4.7 for the static structural analysis was used for a vibration modal analysis. This FEA was completed in ANSYS and was based on the model produced in SolidWorks. An accurate model for structural vibrations within water was reached after modifying the density of the steel of the rackbars and horizontal stiffeners to account for fluid loading. The original density of the steel bars was increased according to Levin’s methodology by adding 0.7 times the specific weight of the fluid times the aspect ratio of the rackbars. Table 10 presents the first fifteen mode shapes identified by the FEA modal analysis.

Table 10: Harmonic frequencies and mode shapes of the trashrack according to the finite element model modal analysis system. The rackbar vibration modes are identified in italics.

Mode	Frequency	Description
1	10.5	Vertical translation of horizontal channels (mode 1)
2	24.5	Translation in the direction of flow (mode 1)
3	28.2	Torsion about middle horizontal channel (mode 1)
4	30.0	Vertical translation of horizontal channels (mode 2)
5	33.6	<i>57" Rackbars (mode 1)</i>
6	35.2	<i>57" Rackbars (mode 2)</i>
7	48.7	Vertical translation of horizontal channels (mode 3)
8	62.7	Quadrant displacements (mode 1)
9	66.2	Translation in the direction of flow (mode 2)
10	68.9	Quadrant displacements (mode 2)
11	72.5	Quadrant displacements (mode 3)
12	78.3	Vertical translation of horizontal channels (mode 4)
13	79.7	<i>28.5" Rackbars</i>
14	79.7	<i>28.5" Rackbars</i>
15	81.6	<i>28.5" Rackbars</i>

The first three frequencies identified in Table 10 are the major structural modes. These are the dominant mode shapes which are repeated throughout the subsequent modes. For example, mode four is the second order shape of mode one. It is significant to notice that there are only four mode shapes in the range of 30 Hz and below. This agrees with the experimental data by suggesting that minimal resonance would occur below the mid-30 Hz range. Furthermore, the excitation of the first four modes would be mechanically difficult because of the high moment of inertia across the trashrack structure. But once mode shapes five and six are reached, the trashrack bars translate in the lateral direction, which

is the least stable direction. Figure 32 is a picture of the displacements associated with the natural frequency of mode five.

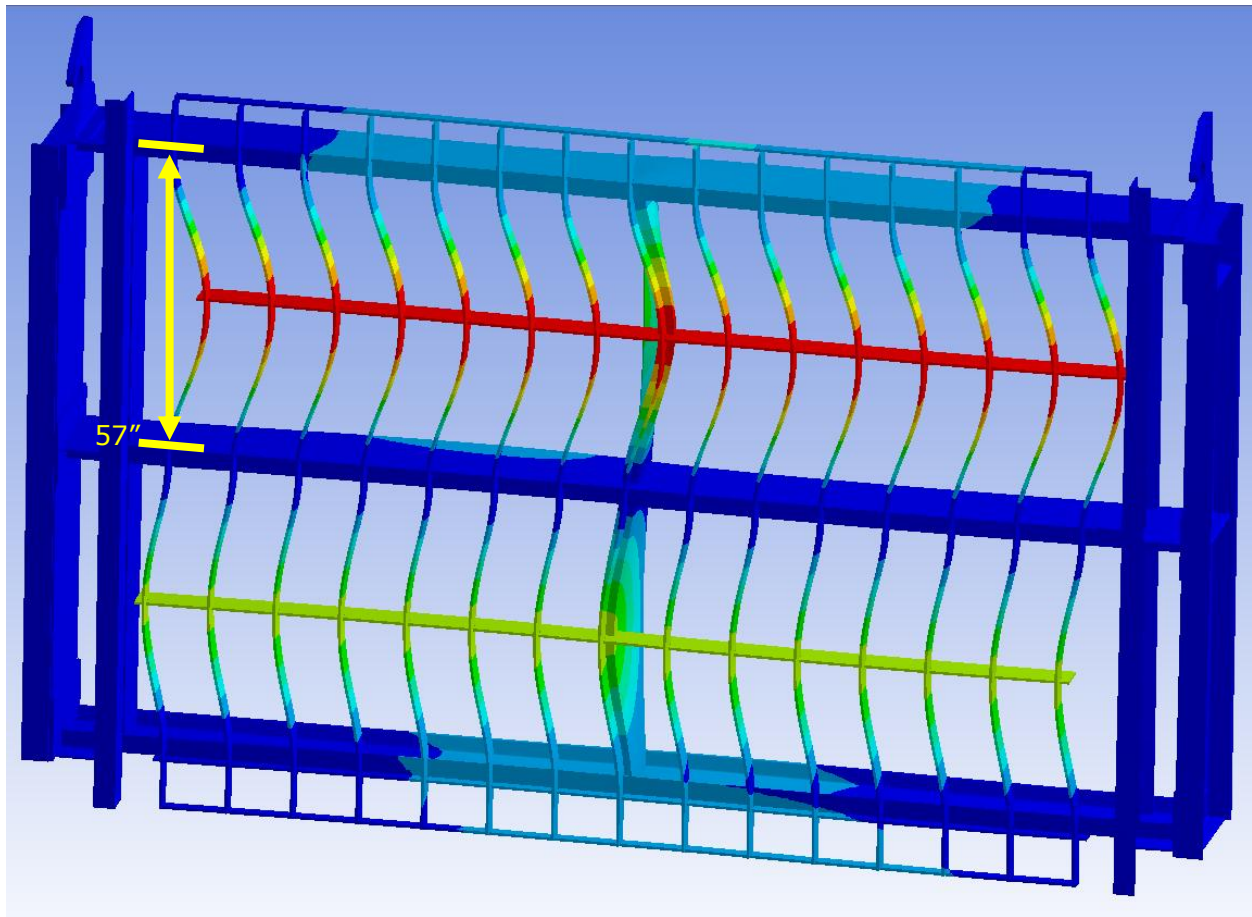


Figure 32: Finite element model vibration mode 5. This is the first resonant frequency of the 57 inch rackbars and occurs at 33.6 Hz.

Both mode five, excited at 33.6 Hz and shown in Figure 32, and mode six, excited at 35.2 Hz, are based on the translation of the 57 inch rackbars. This range is so close to the excitation frequencies observed in the direction of flow and the lateral direction from the experimental data that it is reasonable to accept that the lateral vibrations of the 57 inch rackbars caused the resonance during the physical experiments.

In addition to the relationship between the natural frequencies of the FEA model in the mid-30 Hz range and the experimental data, the vibration calculations also agree with the vibrations of the 57 inch rackbars. This was determined by removing the coupled joint between the center vertical channel and the horizontal support which connects the vertical rackbars. In this modified configuration, the 57 inch unsupported rackbars showed natural

frequencies at 19.0 Hz and 20.2 Hz. A difference of less than ten percent is thus observed between the modified model and Levin's predicted frequency of 21.1 Hz. The same pattern of the model producing a natural frequency just under ten percent of the calculated natural frequency will be examined below for mode shapes involving the single rackbars. The vibrations of the 57 inch rackbars are important because of the transitive relationship between the experimental data, the FEA model, and Levin's original research. The experimental data agrees with the original trashrack model, the modified trashrack model agrees with Levin's calculations, and Levin's calculations agree with the experimental results at 35 Hz.

The next set of natural frequencies presented by the FEA model that exhibit lateral vibrations of the rackbars begins at mode shape 13. These rackbar oscillations begin at 79.7 Hz and mark the onset of the excitation of the 28.5 inch lengths. Only fifteen mode shapes are presented in Table 10, but the model demonstrates the extensive presence of vibrations among the 28.5 inch rackbars concentrated around 80 Hz. Figure 33 displays the lateral displacement of mode 13 at 79.7 Hz.

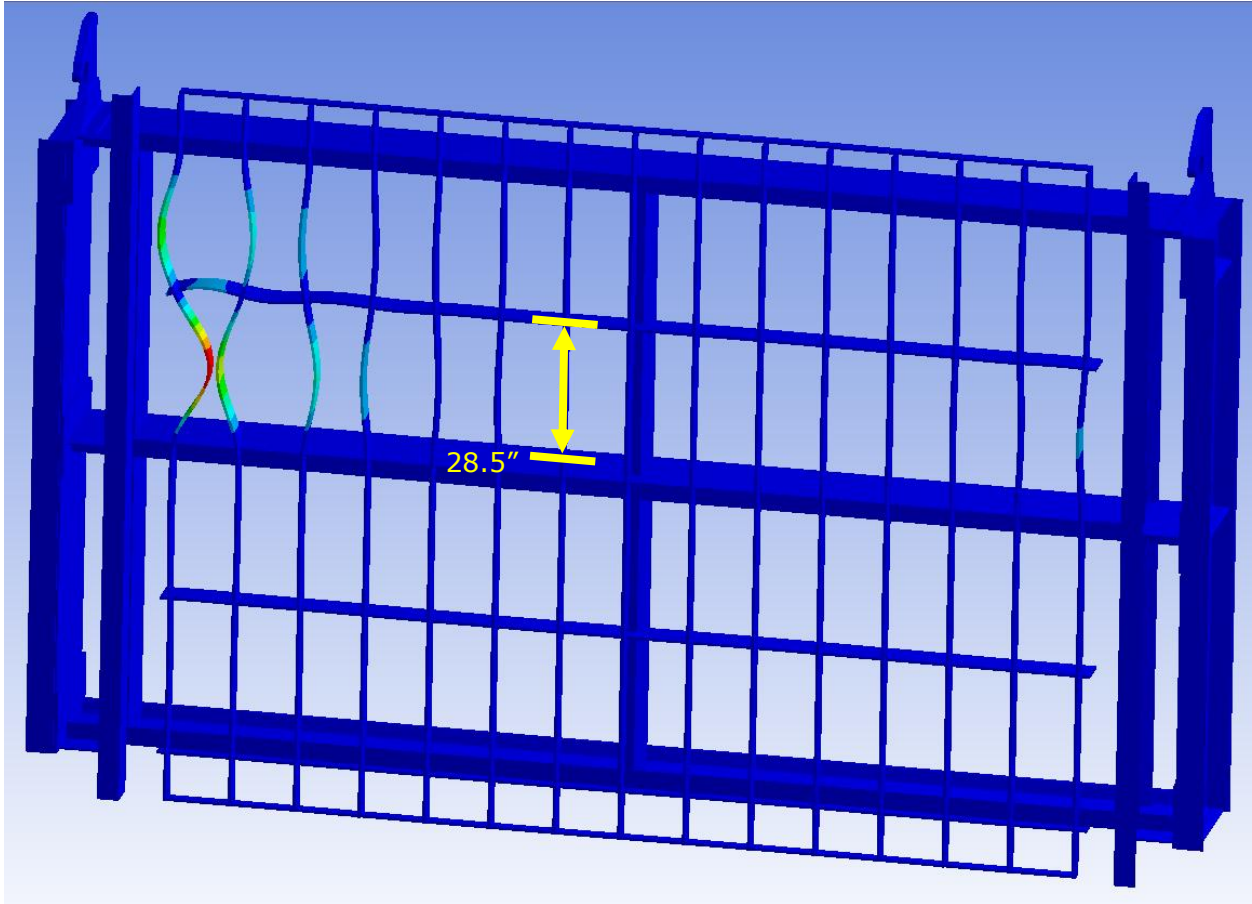


Figure 33: Finite element model vibration mode 13. This is the first resonant frequency of the 28.5 inch rackbars and occurs at 79.7 Hz.

The lowest of these natural frequencies for 28.5 inch rackbars is significant because it is just under ten percent less than Levin's calculated natural frequency. A connection between the results of the model and the calculated natural frequency is obtained by modeling one single rackbar. One 28.5 inch rackbar has a natural frequency of 91 Hz when fixed at both ends. In the real system and in the finite element model the welded connections across the trashrack flex which causes the reported natural frequency to decrease. Accordingly, the calculated natural frequency of the rackbars is within ten percent of both an individually modeled rackbar and the rackbars of an entire trashrack model. Considering that the natural frequencies from the model begin to resonate at a frequency merely 15 percent above the observed 70 Hz experimental response, it is likely that the rackbars are the source of vibrations at the maximum flow rate.

In addition to using the finite element model to obtain the vibration response of the trashrack, it can be used to interpret the differences in magnitude of response for the

accelerometer in all three directions. As viewed in Figure 27 on page 57, the magnitude of the general response in the direction of flow is greater than the magnitude of response in the lateral or vertical directions. This same effect is exhibited in a static structural model of the trashrack when a lateral force is applied to the rackbars. The displacement at the location of the accelerometer is greater in the direction of flow than both the lateral and vertical directions. Similarly, a comparison between each of the displacements in the modal analysis shows that the highest displacements are in the direction of flow when the rackbars are oscillating.

5.4 Vibration Experiments Conclusion

Resonant frequencies at 35 Hz and 70 Hz were identified by the experimental data. The response at 35 Hz is dominant while the flow rate is increasing, but the signal at 70 Hz dominates when the flow has reached the maximum operating condition. Both frequencies are natural frequencies because they are independent of the flow velocity. No dominant velocity dependent frequencies were identified on the experimental data plots.

The response in the mid-30 Hz range is mainly due to the 57 inch rackbar vibrations. A response around 35 Hz is seen in the experimental data and the finite element model. A close correlation between Levin's equation and the finite element model is observed when the density is modified to compensate for the added mass due to the loading of the water. The experimental response of 70 Hz can likely be identified by the lateral movement of 28.5 inch rackbars. These vibrations can be considered the second mode of the 57 inch rackbars. The finite element model predicts a first natural frequency of the rackbars that is fifteen percent above the experimental resonance value. Additionally, Levin's equation yields a natural frequency within 20 percent of the experimental value.

The existence of vibrations at the natural frequencies of the rackbars does not affect the rehabilitation recommendations presented in Chapter 4. The original trashracks were operated for over 60 years, and the field inspections revealed no fractured rackbars. Cracks in some of the rackbar welds were identified, but each of these cracks could be traced to inclusions or undercut in the welds. The maximum stress within the rackbars, exhibited when vibrating at 35 Hz, is 11.5 ksi. This is below the structural fatigue limit of 17.1 ksi. Thus, the analysis concluded that though the rackbars do oscillate at natural frequency

mode shapes, the welding defects are actually the critical source of failure. When the rackbars are properly welded, the lateral vibrations do not reach a destructive limit.

Chapter 6: Conclusions

The trashrack failure analysis case study was a successful collaborative project between Chelan County PUD and the University of Washington. The trashracks at Rock Island Dam were partially modified and prepared for another 40 years of service through the condition assessment and corresponding analysis. A majority of the project was spent verifying that the original design of the trashracks from the 1950s is still sufficient for continued operations. This was accomplished by completing structural, fatigue, vibration, corrosion, welding, and finite element analyses.

The most challenging aspect of the project was handling the shift in focus from a major overhaul to a validation of design. Though the original intent was to modify the rackbar structure to combat vibrations, it became evident that this was not necessary. This realization served the purpose of emphasizing that the field of engineering encompasses much more than just design work. Furthermore, it proved that the exploration of all the potential failure mechanisms is a necessary step for failure analysis projects regardless of the depth of looming repairs.

Another shift in focus was the process of determining the significance of the various failure mechanisms. The project commenced under the hypothesis that vortex shedding vibrations were causing rackbar failures. In the end, the vibrations might have led to the growth of some cracks, but the actual culprit was faulty original welds. These defects created large stress concentrations on the structure which led to the propagation of cracks from the welds. Vibrations of the diagonal tie rods were also identified as a critical failure during the field inspection. These tie rods were replaced with new diagonal braces which were designed to provide the necessary support while withstanding vibrations in the direction of flow and lateral directions.

The ability to repair the existing trashracks rather than completely replace them was a major cost savings for Chelan County PUD. Based on pricing estimates from a similar project completed in 2005, the rehabilitation work cost just over half the price of a set of newly designed and fabricated trashracks. This is a savings of over one million dollars when extrapolating the expenses to the entire set of B5 through B10 trashracks.

Overall the project was a success, but there is always room for improvement is always sought. The two major areas which could have been improved were the collection of the experimental data and the depth of the finite element analysis. Data was gathered from strain gages and an accelerometer, but an ambient signal at 60 Hz rendered the strain gage data virtually useless. The strain gages were originally selected for the project because they were much less expensive and could be used to target localized areas. Unfortunately, they also required tedious installation and the labor expenses eventually tallied four times the cost of the equipment. It thus became apparent that the more expensive purchasing costs associated with the accelerometer could have been easily offset by the ease of installation and reliability of the data. Strain gages might have been implemented properly if the 60 Hz frequency was filtered out during the data collection phase. Additionally, more time could have been spent developing a MATLAB code to filter out the 60 Hz signal. The other main area of improvement could have been the application of the fluid-structural interaction capabilities of ANSYS. The ANSYS Workbench environment allows users to couple fluid dynamics results to structural mechanics solutions. This is a extremely particularly powerful tool which can be used to explore the combined effect of vibration characteristics and structural capabilities within a virtual setting. The scope of the trashrack case study originally included the implementation of the fluid-structural interactions in ANSYS, but the analysis was ultimately condensed to examine the vibrations and static load cases individually.

Looking back on the entire 15 month project, the most important lesson centered on developing a deeper understanding of the importance of properly defining a problem. Establishing clear constraints allows guidelines to be set and goals to be met. Without these boundaries, projects have a tendency to travel aimlessly. This costs both valuable time and money. Within the trashrack failure analysis case study, the first few months were spent focusing on the rackbar vibrations. This proved necessary because it identified the need to focus on other aspects of the trashrack beyond the vibrations. However, time was lost during this initial phase because the observed failures did not match the original description that rackbars were fracturing. A significant, but unintended, accomplishment of this case study is the recognition of the need to properly define engineering problems and establish guidelines at the onset of a project.

Bibliography

- American Institute of Steel Construction. (1991). *Manual of Steel Construction*. Chicago: American Institute of Steel Construction.
- American Society for Testing Materials. (1953). *1952 Book of ASTM Standards: Part 1, Ferrous Metals*. Baltimore: American Society for Testing Materials.
- Blodgett, O. W. (1966). *Design of Welded Structures*. Cleveland: The James F. Lincoln Arc Welding Foundation.
- Bureau of Reclamation. (2009, August 12). *The History of Hydropower Development in the United States*. Retrieved May 2012, from Reclamation, Managing Water in the West: <http://www.usbr.gov/power/edu/history.html>
- Cartier, Lemon, Greenway, Vuong, & Boubnov. (2000). *Turbine Discharge Measurements by Acoustic Sinterillation Flow Meter*. Sidney, B.C.: ASL Environmental Sciences Inc.
- Chelan County PUD. (n.d.). *Rock Island Hydro Project*. Retrieved May 2012, from Chelan County PUD: <http://www.chelanpud.org/rock-island-hydro-project.html>
- Columbia Basin Research. (2012, March). *Hydroelectric Information for Columbia and Snake River Projects*. Retrieved May 2012, from University of Washington School of Aquatic and Fishery Sciences, Columbia Basin Research: <http://www.cbr.washington.edu/crisp/hydro/ris.html>
- Corrosion Control Products Company. (n.d.). *Bitumastic 300M Coal Tar Epoxy Protective Coating*. Retrieved May 2011, from Corrosion Control Products Company: <http://www.farwestcorrosion.com/ccp/protect/carbolin/bitumast.htm>
- CorroView International. (n.d.). *Technical Bulletin C-5: MIC*. Retrieved May 2011, from Corroview: http://www.corrview.com/tech_c_05.htm
- Fontana, M. G. (1976). *Corrosion Engineering*. New York: McGraw-Hill Book Company.
- Fortey, J. W., & Tiry, R. F. (May 1972). Flow-induced transverse vibrations of trashrack bars. *Civil Engineering-ASCE*, 44-45.
- Levin, P. L. (1967). Problemes de Perte de Charge et de Stabilité des Grilles de Prise D'eau. *La Houille Blanche*, 271-278.
- Marin, J. (1962). *Mechanical Behavior of Engineering Materials*. Englewood Cliffs, N.J.: Prentice-Hall.
- Natesan, K. (1980). Corrosion-Erosion Behavior of Materials. *Fall Meeting of The Metallurgical Society of AIME*. New York: The Metallurgical Society of AIME.

- Naudashcher, E., & Wang, Y. (1993). Flow-Induced Vibrations of Prismatic Bodies and Grids of Prisms. *Journal of Fluids and Structures*, 341-373.
- Nguyen, T. D., & Naudascher, E. (1991). Vibration of Beams and Trashracks in Parallel and Inclined Flows. *Journal of Hydraulic Engineering*, 1056-1076.
- Northwest Power and Conservation Council. (n.d.). *Dams: History and Purpose*. Retrieved May 2012, from Northwest Powe and Conservation Council:
<http://www.nwcouncil.org/history/damshistory.asp>
- Oman, P. (n.d.). *The Industrial-Commercial Grade Coal Tar Epoxy Information Page*. Retrieved May 2011, from Epoxy Products: <http://www.epoxyproducts.com/coaltar.html>
- Revie, R. W., & Uhlig, H. H. (2008). *Corrosion and Corrosion Control*. Hoboken: John Wiley & Sons.
- Roberge, P. (n.d.). *Rust Chemistry*. Retrieved May 2011, from Corrosion Doctors: <http://www.corrosion-doctors.org/Experiments/rust-chemistry.htm>
- Sell, L. E. (1971). Hydroelectric Power Plant Trashrack Design. *Journal of hte Power Division, Proceedings of hte American Society of Civil Engineers*, 115-121.
- Shigley, J. E. (n.d.). *Mechanical Engineering Design* (Eighth ed.). McGraw-Hill.

Acknowledgements

My thesis project is similar to other students' projects in that it required a significant amount of external support. From theory, to purchasing, to general execution, many people played a valuable role in the success of my project. I would first like to thank the following people at the University of Washington:

- Dr. Reinhall...for providing overall project guidance, finite element modeling direction, and assisting in the interpretation of my data. As the chair of my committee, he kept me honest and on track while ensuring my project concluded as a success.
- Bill Kuykendall...for guidance in the selection of my accelerometer and strain gage equipment, the hands on tutorials to ensure I knew how to operate the equipment, and the generous agreement to let me borrow equipment.
- Dr. Sandwith...for providing the backbone of the corrosion analysis through his corrosion class, and for agreeing to be a member of my thesis committee.
- Dr. Dahl...for agreeing to be a member of my thesis committee.
- Sue Chen...for ensuring that all of my budget concerns were quickly resolved.

I would also like to thank the following people at Chelan County PUD:

- Brett Bickford...for everything. He was open to the UW—PUD partnership, helped me jump through hoops at both organizations, and provided excellent guidance throughout the project while serving as an exemplary leader in the office environment.
- Travis Dolge...for hours of overtime spent in the hot sun applying and wiring the experimental equipment.
- Mike McCarl...for coordinating the field inspections and repairs performed by the mechanics at Rock Island Dam.
- Bret Stone, Dave Stedman, Vince Norton, Rick Jackson...for the countless weeks spent lifting, transporting, cleaning, grinding, cutting, repairing, and welding the trashracks to ensure they were properly examined and repaired.
- Chuck...for his insight on the daily grind. Chuck taught me more about the applied world of engineering than I ever learned in a classroom because he taught me how to work and communicate with those around me.

Finally, I owe a huge thanks to my parents and my friends. They supported me along the frustrating process of completing a thesis and never failed to offer reassurance that I would eventually finish the project. My closing words of appreciation are extended to my mother for reminding me how to properly diagram a sentence.

Appendix A: Original Design Specifications

The original Invitation for Bids and design specification are included in the next eight pages. Stone and Webster released both the bidding document and design criteria for the trashracks at Rock Island Dam in 1951. W.H. Reller was awarded the contract and completed the fabrication work in 1953. Drawings 8591-FH-43 and 8591-FH-3576 were provided by Stone and Webster to W.H. Reller for the manufacturing process. W.H. Reller compiled shop drawings labeled 137-1, 137-2, 137-3, 137-4, 137-5, 137-6, and 137-7. None of the original drawings are provided because they are of poor quality and cannot be interpreted on 8.5 inch by 11 inch paper. The most notable criterion included in the design specification document is that the trashracks must support a hydrostatic head of five feet.

INVITATION FOR BIDS

ON

TRASH RACKS

ROCK ISLAND HYDRO-ELECTRIC PRODUCTION SYSTEM
PUBLIC UTILITY DISTRICT NO. 1 OF
CHELAN COUNTY, WASHINGTON

STONE & WEBSTER ENGINEERING CORPORATION, Engineers

Boston, Massachusetts, September 10, 1951
(City, State) (Date)

1. GENERAL.

Bids will be received at the office of Stone & Webster Engineering Corporation, 49 Federal St., Boston, Massachusetts up to October 15, 1951 for the items included in the specifications attached hereto dated September 10, 1951 and the drawings listed therein or attached thereto.

The right is reserved to reject any or all bids.

The successful bidder will be required to enter into a written contract with the Purchaser for the performance of the work included in the drawings and specifications. This contract will be the standard form used by the Engineers, an abstract of which is attached hereto.

2. FORM OF PROPOSAL.

Bidders are requested to submit a proposal on a lump sum basis for furnishing all labor and material in accordance with the Engineers' drawings and specifications. Blank spaces in the Purchaser's specifications must be filled in with the data called for and any other information that may be requested must be supplied.

Bidders are requested to furnish an original and 3 copies of their proposal.

~~Bidders are requested to state explicitly the field labor conditions on which their proposals are based, including the sources of labor.~~
(see below)

3. COMPLETION OF WORK.

Bidders shall state the number of weeks or calendar days following receipt of order which will be required to make shipment of equipment specified.

4. TIME AND MANNER OF PAYMENTS.

To be stated by Bidders.

2. FORM OF PROPOSAL (CONT'D)

Prices shall be for finished equipment, fob cars Bidder's works with freight allowed to destination.

In addition to the lump sum price, Bidders shall state separate prices for each of the two items specified.

5. RAILROAD FACILITIES.

Equipment will be hauled by Purchaser from railroad siding to job site.

6. UNLOADING.

The Contractor shall erect pile-store material delivered by the Contractor. Purchaser will unload, haul and store. Purchaser will assume all responsibility for care and protection of same after unloading. transfer or issuance to him by the Purchaser.

7. WATER. (Not required)

Water will be available at the site without charge at current rates.

8. COMPRESSED AIR. (Not required)

Compressed air at approximately psi will be available at the site without charge to the extent authorized by the Engineers' Superintendent of Construction.

9. ELECTRIC POWER. (Not required)

Electric power will be available at the site without charge at current rates to the extent authorized by the Engineers' Superintendent of Construction as follows: volts, a-c, cycles, phase. volts, a-c, cycles, phase.

10. CRANES. (Not required)

crane of capacity will be available for the Contractor's use. No charge will be made for use of the crane or for power. The Purchaser will provide a competent operator for the crane whose services will be charged to the Contractor.

11. SERVICE CONNECTIONS. (Not required)

The Contractor shall make, maintain and remove his own connections at the Purchaser's or other points of supply and also provide and maintain his own piping and/or wiring for all water, air, electric power and other services required for his erection work.

12. LICENSE LAWS.

The Contractor shall comply with the requirements of any applicable State or Local laws with respect to the licensing of Contractors.

13. FIELD LABOR. (Not required)

The Contractor shall employ such field labor as will cause no conflict or interference with other trades.

ABSTRACT OF ENGINEERS' FORM OF CONTRACT

The contract which the successful Bidder will be required to sign will contain clauses relating to the following:

1. The contract and specifications, with drawings, if any, shall be considered together so that any work shown on drawings, though not mentioned in the contract and specifications, or vice versa, shall be executed as a part of this contract. The Contractor's specifications shall be supplementary to the Purchaser's and in case of discrepancy between them, the latter shall take precedence.
2. The Purchaser may increase or decrease the amount of work or make alterations, giving the Contractor a written order. No claim for additional compensation will be allowed unless covered by such an order. Unless otherwise specified, extras will be paid for only on the basis of an audited cost plus an allowance to cover profit.
3. The Contractor shall complete the work within the time specified in the contract, or as extended by written order unless delayed by strikes or other unavoidable causes.
4. The Contractor shall prosecute the work continuously in such a manner and in such order of precedence as may be directed, working overtime, if necessary, to meet the specified date of shipment or erection, without claim for extra expense caused thereby.
5. If alterations or additions to work or delays not the fault of the Contractor require an extension of time for completion of contract, it shall be allowed if claim is made in writing to the Engineers and approved in writing by them.
6. The Contractor shall hold harmless the Purchaser and his agents from damages for patent infringement.
7. The Contractor shall guarantee that the apparatus included in the contract and specifications shall be free from all inherent defects in design, workmanship, or material and shall give proper and continuous service under all the conditions of service required and specified or which may be reasonably inferred from the specifications, and that all work performed by him shall be perfect in material and workmanship.
8. The Contractor shall agree to repair or replace, at his own expense, any part of the apparatus, materials, or workmanship proving defective within.....one year.....after date of acceptance.
9. The Contractor shall obtain prior approval of the Purchaser before entering into sub-contracts for any part of the work.
10. Liquidated damages may be required for failure to complete the work by the date stated, with provision for any extension of time granted by written permission from the Engineers.
11. The Contractor may be required to furnish a Surety Bond for the faithful performance of his work. Unless otherwise specified the cost of the bond shall not be included in the bid but will be added to the bid if the bond is required.
12. Before any of his employees shall do any work upon the premises under the control of the Engineers, the Contractor shall provide for the payment of Workmen's Compensation benefits to his employees or their dependents in accordance with the laws of the state in which the work is performed and all amendments thereto, and shall also carry a Public Liability policy, with limits of at least \$25,000 for any one person and \$50,000 for any one accident.
13. The Contractor shall conform to all local, state and Federal regulations and secure and pay for all necessary permits.
14. The Contractor will be responsible for the work until fully completed and accepted, irrespective of whether advance payments have been made.
15. The Contractor shall hold harmless the Purchaser and his agents from loss or damage resulting from action or neglect of the Contractor or his employees or agents.
16. Provision will be made for arbitration of items in dispute between the Contractor and Purchaser.

S P E C I F I C A T I O N

FOR

TRASH RACKS

FOR

ROCK ISLAND HYDRO-ELECTRIC PRODUCTION SYSTEM

FOR

PUBLIC UTILITY DISTRICT NO. 1
OF CHELAN COUNTY, WASHINGTON

Stone & Webster Eng. Corp., Engrs. Boston, Mass., September 10, 1951

GENERAL

This specification covers the general requirements for materials, fabrication and delivery for the manufacturer's plant with freight allowed to destination, for trash racks, as described herein.

The Contractor shall provide all labor, materials, tools, equipment and plant that may be required for performing the work with first class workmanship and in a manner satisfactory to the Engineers.

The Contractor shall completely assemble and shop coat the racks as specified herein before shipment. With bracing rods drawn up tight the racks shall be square, true to dimensions and free from twists.

WORK INCLUDED

The work included in this specification is shown on the Engineers' drawings and comprises the following principal items:

- Item 1 - Fifty-four rack sections with steel rack bars
- Item 2 - Fifty-four rack sections with timber facing

WORK NOT INCLUDED

- a. Guides for trash racks
- b. Anchor bolts, sleeves and washers
- c. Field erection

TYPE OF SERVICE

The racks will be used to remove coarse trash which may accumulate in front of the power station intakes. The steel sections will be located directly in front of the openings and the timber faced sections will be placed above the steel sections behind the fender wall to provide a continuous vertical surface against which the trash may be brought to the top of the upper timber section by a trash rake. The trash rake equipment will include a timber faced apron which, when lowered into place above the permanent racks, will extend the raking surface to deck level. All sections are designed to withstand an unbalanced hydrostatic head of 5 ft. The steel sections will be completely submerged at all times.

The rack sections will be lowered and raised by special sheaves and lifting hooks carried by the gantry crane running on the deck of the intake section. These hooks will pick up or deposit the rack sections underwater, each section being provided with two lifting hooks for this purpose. Trash will be removed from the racks by a mechanical rake arranged to travel parallel to the face of the racks. The rake will be handled by a hoist operating from the gantry crane.

ENGINEERS' DRAWINGS

The Engineers' drawings applying to the work included under this specification are as follows:

- 8591-FH-43 - Trash Racks - Main Units - Rev. 1
- 8591-FH-3576 - Trash Rack and Stop Log Guides

These drawings show the work in sufficient detail for the preparation of shop drawings by the Contractor.

Engineers' drawings are in general to scale but figured dimensions shall always be followed. In case of errors or omission of dimensions the Engineers shall be consulted.

SHOP DRAWINGS

As soon as practicable after the awarding of contract, the Contractor shall furnish three prints of all shop details and assembly drawings. The Engineers will return one print of each

drawing to the Contractor marked "Returned for Revision", "Approved as Revised" or "Approved". Revisions shall be made promptly and three additional prints furnished to the Engineers. Drawings marked "Approved" or revised in accordance with prints marked "Approved as Revised" may be placed at once in the shop. Upon receipt of drawings marked "Approved", the Contractor shall promptly furnish the Engineers with nine additional prints.

The Engineers' approval shall apply to general arrangement and shall not relieve the Contractor from responsibility for the correctness of details and dimensions. Any fabrication or other work done in advance of receipt of approved shop drawings will be entirely at the risk of the Contractor.

MATERIALS

All material designations refer to current issues.

Structural Steel	ASTM-A7
Bar Steel	ASTM-A-107
Wrought Iron	ASTM-A-84
Coal Tar Enamel	AWWA-7A-5

Machine steel shall be of a good commercial grade containing 0.35% to 0.45% carbon and having an ultimate tensile strength of 70,000 to 80,000 psi.

All trash rack facing timbers shall be sound dense select Douglas fir, as indicated on the drawings, well seasoned and free from season cracks or knots.

All materials shall be of the best of their respective kinds; shall conform to the chemical and physical tests and grading of the specification designations given above.

SUBSTITUTIONS

Nuts and bolts can be hot galvanized steel in lieu of hot galvanized wrought iron.

Square edged flats may be substituted for round edge flats if the latter are not obtainable.

WELDING

All welding shall conform to the current issue of the Building Code of the American Welding Society.

40

Welding shall be done by operators who have been previously qualified by tests as prescribed in the American Welding Society Standard Qualification Procedure to perform the type of work required.

Welding equipment shall be of a type which will produce and maintain the proper current so that the operator may produce satisfactory welds.

All welds shall be made by the electric arc method.

Welding rods shall be coated electrodes of material similar to that of the parts being welded.

The appearance and quality of welds made, and the method of correcting defective work shall conform to the American Welding Society Code for electric arc welding.

Surfaces to be welded shall be free from loose scale, dust, grease, paint and other foreign material.

FABRICATION

All workmanship shall conform to the best modern shop practice. Rack sections shall be shop fabricated, and shipped complete.

Each rack section shall be carefully squared, and the front edge of all rack bars shall be on one plane. Side members shall be parallel and normal to cross members.

To prevent undue twist and warp due to welded connections, the assemblage during welding shall be securely held in a strong jig and when the completed work is released therefrom any resulting twist or warp shall be removed by applications of heat and pressure. Hammering will not be permitted. Where the warp or twist is slight, peening will be permitted provided the worker is skilled in the art. Inspection shall be made for cracked welds, which if found, shall be corrected by removing defective weld metal and rewelding with new metal.

All surfaces of rack bars and other surfaces to be in contact with guides shall be free of all burrs, extended welds or projections of any kind that may interfere with the ease of operation. Ragged or sharp edges on any and all members shall be removed.

The slots in the plates which support the trash rack bars shall be clean cut and accurately spaced so that the bars will be in a straight line and evenly spaced. The slots shall be such as to be a good fit around the rack bars so that minimum welding will be necessary to hold them in place.

The lifting hooks shall be layed out accurately by template and carefully fabricated so that on all trash racks they will be spaced alike, in their correct position in relation to the lifting hooks.

The centering pins and centering guides shall be accurately located to assure a perfect vertical alignment of the racks.

All timbers shall be milled to the sizes shown on the drawings. Surfacing shall be done by machine. All bolt holes and counterbores shall be accurately located, preferably to template.

All bolts and nuts shall be hot galvanized after threading. The threads on the bolts and nuts shall have sufficient clearance to allow for the coating of zinc. Threads may be cut or rolled. All bolts shall have square heads and full-sized shanks. All nuts shall be hexagonal.

All equipment shall be completely assembled in the shop, and inspected. Any errors disclosed shall be corrected by grinding, remachining or by furnishing new parts, as may be necessary or ordered by the inspector. All unfinished surfaces adjoining finished surfaces shall be chipped, filled or ground to remove projecting corners, fins or rough edges.

PAINTING

After inspection and shop erection, all structural steel surfaces to be painted shall be flame-cleaned followed immediately by wire brushing and dusting and then, while the steel is still warm or before condensation begins, a priming coat of coal tar enamel shall be applied. When the priming coat has been dried and becomes hard to the touch, a finish coat of hot enamel shall be applied. Coal tar enamel primer and coal tar enamel shall meet the requirements of American Water Works Association Specification 7A-5 and shall be applied according to the applicable sections of the same specification.

SHOP INSPECTION

The Contractor shall cooperate with the Purchaser in furnishing facilities for inspecting and testing both the weight of material and quality of workmanship at the mill or shop. Inspection will be made by an inspector designated by the Engineers. He shall have full access at all times to all parts of the mills or shops where work to be inspected by him is being rolled or fabricated. He shall be furnished with all facilities for

Appendix B: MWH Evaluation Report (2005)

MWH conducted a condition assessment of the B5 through B10 trashracks in the summer of 2005. The initial physical inspection of the trashracks was performed in June. The final evaluation report, which included structural calculations, vibration characteristics, and an assessment of the visual condition of the trashracks, was completed in August.

The report was intended to be phase one of a two-phase project. Phase one included the initial inspection and assessment of the existing trashrack design. Phase two was outlined to be a rehabilitation study which would be initiated if it was determined that rehabilitation work was necessary and if it would be economical to repair the racks rather than replace them. The executive summary, part of the original fifteen page evaluation report, is highlighted in yellow over the next two pages.

Engineering Services Evaluation Report - Feasibility

1.0 Executive Summary

The work under Task Authorization No. 82 relates to a review of the existing trashracks at Rock Island Powerhouse No. 1 Intake B5 to B10 to determine acceptability with respect to their current condition, structural integrity, and hydraulic performance. The following highlights of the report are as follows:

1. The rackbar spacing (the existing rackbar spacing is 12-in. o.c.) is assumed to be acceptable for the new turbine units to be supplied by VA Tech. Per the District's Randy Walter, the turbine supplier was provided with information on the existing racks during their machine design, therefore the acceptability of the present rack spacing was their responsibility to confirm. Randy Walter also confirmed with VA Tech that the 12-in. spacing was acceptable.
2. Based on the results of the 2005 inspection and structural analysis, there is no immediate concern regarding the structural integrity of the trashracks for the new flow rate of 9000 cfs provided the differential head across the trashrack panels is not permitted to exceed 5-ft. It is recommended, however, that the trashracks be strengthened in the near future to increase their ability to accommodate head differentials up to 10-ft. in case of a significant debris buildup. A 10-ft. head differential is commonly used for the design of new trashracks and is considered a safe design loading for the expected conditions at the project.
3. For the new maximum flow rate of 9000 cfs, the safety factor against resonance due to flow induced vibrations has been evaluated to be less than the normally acceptable value. (Assuming no corrosion, the computed value was 2.09 vs. an industry accepted standard of 2.5). If significant uniform corrosion was present on the racks, this value could continue to drop to unacceptable levels. The inspection, however, indicated corrosion on the rack bars to be generally minimal, therefore a safety factor of 2.09 is considered acceptable for the short term but should be increased to the recommended value to meet the acceptable design criteria for the long term operation of the project. In order to increase the factor of safety, the effective unsupported length of the rack bars should be reduced.
4. No modifications appear to be viable to significantly improve the hydraulic performance. The hydraulic losses across the trashracks were calculated to be minimal.
5. It is recommended that the trashracks in at least two additional working bays be removed and inspected prior to initiating design of rehabilitation measures. It would be preferable to inspect the trashrack sections in the bays that have historically accumulated the most debris over the years. The inspection, in

Engineering Services Evaluation Report - Feasibility

this case, would provide more relevant information on deformation, condition of the paint coating system, consistency of corrosion loss on the members (rack bars and main horizontal support members), and will assist in the verification of assumptions made in the report with respect to adequacy.

6. Additional recommendations with respect to the eventual rehabilitation of the trashracks are provided in the report. The report also briefly discusses debris handling options.

2.0 Justification

Keeping with the overall rehabilitation plan to modernize the existing hydro generation system to increase efficiency and to verify sufficient protection to the new Units against damage from debris, the District has issued a task order to study the structural and hydraulic adequacy of the existing trashracks. The primary focus of the study is to determine what, if anything needs to be done to the existing trashracks to raise them to modern-day design standards. The secondary purpose of the study is to determine whether significant improvements can be made with respect to hydraulic efficiency that may economically justify modification or replacement of the rack system to increase overall hydrogeneration efficiency.

3.0 Scope of Work

The scope of work is being handled in two phases. The first phase will include a cursory inspection and assessment of the accessible trashracks and a performance review to determine whether they are structurally acceptable for continued usage. Phase 2 of the study, will be a rehabilitation study to develop a plan for the rehabilitation of the trashracks if it is determined they can be rehabilitated. If new trashracks are needed, the District will initiate steps to procure new trashracks.

Phase 1 work includes the following:

- Collection and Review of Existing Data. Collect and review existing drawings and data for the B5 through B10 trashracks.
- Kickoff Meeting and Inspection. Meet with District engineers to discuss the objectives of the study and to collect the necessary data, drawings and other applicable information. Inspect the six existing PH1 trashrack sections stored in the PH2 yard. (These were removed from Unit B7 or B8) to assess the present condition of the racks and estimate the level of deterioration to be

Appendix C: Calculations

Calculations are presented in this appendix for the static structural analysis, the fatigue analysis, the vibration analysis, and the replacement design for the tie rods.

C.1 Static Structural Calculations

Static structural calculations were performed according to a general mechanics of materials approach. The bending equation was applied to the rackbars and the horizontal structural beams of the trashrack. As specified by the original design documents, each trashrack was required to support a static head of five feet. A pinned-pinned condition was assumed which is the most conservative approach. Corrosion was introduced as a percentage of reduction to the cross sectional area and factored into the section modulus. The American Institute of Steel Construction (AISC) convention of accepting 60% of the yield strength as the maximum operating limit was followed for the trashrack analysis.²⁹ Accordingly, 18 ksi was the allowable stress level when assessing the strength of the A30 structural members. Table 11 and Equations C.1 through C.7 present the parameters used for the structural calculations.

Table 11: Parameters for structural calculations.

Description	Variable	Units
Head	Δz	ft
Span	l	in
Spacing	d	in
Thickness	T	in
Width	W	in
Section modulus	S	in ³
Pressure	Δp	psi
Distributed load	w	lbf/ft
Bending moment	M	lbf-ft
Shear force	V	Lbf
Shear stress	τ	Ksi
Bending stress	σ	ksi

²⁹ (American Institute of Steel Construction, 1991)

$$S = \frac{1}{6} T \cdot W^2 \quad [C.1]$$

$$\Delta p = \gamma \cdot \Delta z \quad [C.2]$$

$$w = \Delta p \cdot d \quad [C.3]$$

$$M = \frac{wl^2}{8} \quad [C.4]$$

$$V = \frac{wl}{2} \quad [C.5]$$

$$\tau = \frac{V}{A} \quad [C.6]$$

$$\sigma = \frac{M}{S} \quad [C.7]$$

Table 12 applies the design criteria to the parameters identified above to solve for the operating stresses in the rackbars. The stresses on the rackbars are very low which indicates that the load of the water or accumulation of debris on the trashracks would not cause the rackbars to break. Table 13 and Table 14 present the same set of calculations for the top and middle horizontal structural channels.

Table 12: Static structural calculations for the rackbars of the trashrack at varying loads and corrosion.

Description	Units	Config. 1	Config. 2	Config. 3	Config. 4
Corrosion	%	0	0	10	10
Head	ft	5	10	5	10
Span	ft	28.875	28.875	28.875	28.875
Spacing	in	12	12	12	12
Thickness	in	0.5	0.5	0.5	0.5
Width	in	4	4	4	4
Section Modulus	in ³	1.33	1.33	1.20	1.20
Load	lbf/ft	312	624	312	624
Bending Moment	lbf-ft	226	452	226	452
Shear Force	lbf	375	751	375	751
Shear Stress	ksi	0.2	0.4	0.2	0.4
Bending Stress	ksi	2.0	4.1	2.3	4.5

Table 13: Static structural calculations for the top beam of a trashrack at varying loads and corrosion.

Description	Units	Config. 1	Config. 2	Config. 3	Config. 4
Corrosion	%	0	0	10	10
Head	ft	5	10	5	10
Section Modulus	in ³	42	42	37.8	37.8
Area of Cross Section	in ²	9.96	9.96	9.96	9.96
Span of Top Beam	ft	17.2	17.2	17.2	17.2
Loading Strip Width	in	38.375	38.375	38.375	38.375
Load on Top Beam	lbf/ft	998	1,996	998	1,996
Bending Moment	lbf-ft	36,897	73,794	36,897	73,794
Shear Force	lbf	8,581	17,161	8,581	17,161
Shear Stress	ksi	0.9	1.7	1.0	1.9
Bending Stress	ksi	10.5	21.1	11.7	23.4

Table 14: Static structural calculations for the middle beam of the trashrack at varying loads and corrosion.

Description	Units	Config. 1	Config. 2	Config. 3	Config. 4
Corrosion	%	0	0	10	10
Head	ft	5	10	5	10
Section Modulus	in ³	42	42	37.8	37.8
Area of Cross Section	in ²	9.96	9.96	9.96	9.96
Span of Top Beam	ft	17.2	17.2	17.2	17.2
Loading Strip Width	in	58.50	58.50	58.50	58.50
Load on Top Beam	lbf/ft	1,521	3,042	1,521	3,042
Bending Moment	lbf-ft	56,247	112,493	56,247	112,493
Shear Force	lbf	13,081	26,161	13,081	26,161
Shear Stress	ksi	1.3	2.6	1.5	2.9
Bending Stress	ksi	16.1	32.1	17.9	35.7

A comparison between the top beam and the middle beam validates that the middle beam experiences higher stresses because the loaded area is about 50 percent greater. The calculations also show that the stress of the middle beam rises above the allowable limit of 18 ksi between a head of five feet and ten feet. The introduction of 10% corrosion to the middle beam demonstrates that the allowable stress limit is effectively met at a head of five feet. It can be summarized from these calculations that the trashracks are properly designed for a head of five feet, but should not be operated above this limit.

C.2 Fatigue Calculations

Fatigue calculations were performed to determine the maximum allowable stress level for the A30 steel trashracks. This stress limit was used to analyze the structural beams and the rackbars of the trashracks. Table 15 walks through Shigley’s application of the Marin equation³⁰:

$$S_e = k_a k_b k_c k_d k_e k_f S_e' \quad [C.8]$$

Table 15: Endurance limit calculations for A30 steel.

Variable	Quantity	Units	Description
σ_{UT}	55	ksi	Ultimate tensile strength of A30
S_e'	27.5	ksi	Rotary-beam test specimen endurance limit: $S_e' = 0.5\sigma_{UT}$
k_a	0.89	-	Surface factor for hot rolled: $k_a = a\sigma_{UT}^b$, $a=14.4$, $b=-0.718$
k_b	0.70	-	Size factor for bending: $k_b = 1.51d^{-0.157}$, for $51 < d \leq 254 \text{ mm}$, where $d_{effective} = 136 \text{ mm}$
k_c	1	-	Loading factor for bending
k_d	1	-	Temperature factor for less than 65 degrees Fahrenheit
k_e	NA	-	Reliability factor, no information available
k_f	NA	-	Miscellaneous effects factor, no information available
S_e	17.1	ksi	Modified endurance limit for A30

The trashracks are currently 60 years old, and this rehabilitation project was conducted to provide another 40 years of service. Throughout the desired 100 year life span, the trashracks would have to be loaded and unloaded 27 times per day to reach one million cycles. One million cycles is commonly accepted as the number of stress cycles for infinite life of steel components. Considering that the endurance limit for A30 is 17.1 ksi, which is relatively close to the maximum stress of 16.1 ksi in the middle beam, it is fortunate that the trashrack is not continuously loaded and unloaded. A more realistic estimate is that the trashrack is loaded and unloaded an average of once or twice per day, resulting in less than 60,000 cycles over the 100 years. For this reason, the allowable stress limit is safely above 17.1 ksi.

The fatigue limit was not applied to the rackbars because the operating stresses are well below the allowable limit of 17.1 ksi for the A30 steel trashracks.

³⁰ (Marin, 1962)

C.3 Vibration Calculations

Vibrations of the rackbars on the trashrack were analyzed according to the method developed by Levin.³¹ This includes a comparison of the forcing frequency from the flow of the river to the natural frequency of the bars on the trashrack. A factor of safety of 2.5 is desired for the rackbars according to Levin.

Developing an understanding of the flow through the turbine and trashracks was the first step in calculating the fluid-induced vibrations. Table 16 presents the cross-sectional flow area for one trashrack. A reduction in area is presented at the beginning of Table 17, which was calculated from the gross and net flow dimensions of an individual trashrack. Table 17 uses this reduction in area to determine the net flow area through one intake bay. The net flow area for the intake bay is necessary to determine the flow velocity of the water as it passes through the trashrack. Finally, differentiating between units B5 and B6 and units B7 through B10 is important because their intake heights are not the same. This is important when calculating the forcing frequency which is derived from the flow rate of the water.

Table 16: Gross and net flow dimensions for a single trashrack.

	Trashrack gross flow dimensions		Trashrack net flow dimensions	
Width	184 in	15.3 ft	174 in	14.5 ft
Height	136 in	11.3 ft	122.3 in	10.2 ft
Area	25,024 in ²	174 ft ²	21,280 in ²	148 ft ²

Table 17: Net flow area for one intake bay at the turbine.

Description	B5 & B6	B7-B10	Units
Reduction	15%	15%	-
Total intake height	30.4	34.5	ft
Gross flow area	466	529	ft ²
Net flow area	396	450	ft ²

The current operating flow rate through the turbine is 7,800 cubic feet per second (cfs). However, a flow rate of 9,000 cfs was also analyzed as the maximum flow condition which would exist in the event of turbine runaway. Of the three intake bays for each turbine, the north bay receives 39% of the total flow. This is due to the shape of the scroll case. Furthermore, approximately 10% of the flow passes through the top three wood trashracks.

³¹ (Fortey & Tiry, May 1972)

Combined, these two modifying factors reduce the 7,800 cfs flow and 9,000 cfs flow to 2,738 cfs and 3,159 cfs, respectively.

Strouhal’s forcing frequency method was used to determine the vibrations from the flow of the river. Vibrations among the rackbars are a result of the formation of alternating high and low pressure regions, known as vortex shedding, at the trailing edge of the rackbars. Table 18 (units B5-B6) and Table 19 (units B7-B10) present the results of the Strouhal calculations which characterize the oscillations of the rectangular bars due to the vortex shedding. It is important to differentiate between units B5 and B6 and B7 through B10 because of the difference in net flow area.

Table 18: Rackbar vibration forcing frequency calculations for turbines B5 and B6.

Forcing frequency, $ff = S \times V / t$

Variable	Quantity (7,800 cfs flow)	Quantity (9,000 cfs flow)	Units	Description
t	0.5	0.5	inch	thickness of bar perpendicular to flow
b	4	4	inch	depth of bar in flow direction
s	0.216	0.216	NA	Strouhal number = $0.12 + 0.012 \times b / t$
Q	2738	3159	cfs	flow, reduced to 90%
A	396	396	sq ft	net flow area
V	82.9	95.6	in/s	average velocity
ff	35.8	41.3	Hz	forcing frequency

Table 19: Rackbar vibration forcing frequency for turbines B7 through B10.

Forcing frequency, $ff = S \times V / t$

Variable	Quantity (7,800 cfs flow)	Quantity (9,000 cfs flow)	Units	Description
t	0.5	0.5	inch	thickness of bar perpendicular to flow
b	4	4	inch	depth of bar in flow direction
s	0.216	0.216	NA	Strouhal number = $0.12 + 0.012 \times b / t$
Q	2738	3159	cfs	flow, reduced to 90%
A	450	450	sq ft	net flow area
V	73.0	84.3	in/s	average velocity
ff	31.5	36.4	Hz	forcing frequency

Levin’s harmonic frequency calculations are implemented in Table 20 (units B5-B10). The harmonic frequency of the rackbars is the same for all the trashracks because the steel structures have the same geometry from units B5 through B10.

Table 20: Rackbar natural frequency for units B5 through B10.

Natural Frequency of Rackbars, $f_n = K \times r / L^2 [g \times E / (Wb + 0.7 * b / t)]^{0.5}$

Variable	Quantity	Units	Description
K	3.56	NA	Coefficient for fixed ends
t	0.5	inch	length of bar perpendicular to flow
b	4	inch	length of side of bar parallel to flow
r	0.144	inch	radius of gyration of the bar about an axis parallel to long side
L	30.6	inch	length of bar between supports, multiplied by 1.07 for half notch connection
g	386	in/s ²	acceleration due to gravity
E	3.00E+07	psi	Young's modulus of bar material
Wb	0.286	lb/in ³	specific weight of bar material
Wf	0.036	lb/in ³	specific weight of fluid
f _n	84.5	Hz	natural frequency

All the vibration calculations are targeted at producing two numbers; the forcing frequency due to the flow and the factor of safety against the harmonic frequency of the structure. Table 21 summarizes the calculations for the operating flow conditions and runaway flow conditions for each of the units.

Table 21: Vortex shedding vibration calculation summary.

Description	Summary of Calculations			
	5 & 6		7 to 10	
Unit				
Flow rate into turbine (cfs)	7,800	9,000	7,800	9,000
Natural frequency (Hz)	84.5	84.5	84.5	84.5
Forcing frequency (Hz)	35.8	41.3	31.5	36.4
Factor of safety	2.4	2.0	2.7	2.3

C.4 Welding Calculations

The hydrostatic structural calculations from Appendix A1.2 determined that the middle beam experiences the highest stress on the trashrack. Consequently, the welds supporting the middle beam are the most critical. Blodgett's method of treating the weld as a line was selected for the welding analysis. His approach determines the required weld size based on the force of a combined loading situation and the equivalent length of the weld.

A single fillet weld extends continuously around the middle beam. It has a leg size of at least one-eighth inch in all locations. The electrode used to manufacture the trashracks was unknown, so an E60 electrode was used for the analysis because it is the most conservative choice. An E60 electrode has a weld strength of 9,600 psi. A list of the parameters and calculations for the analysis is provided in Table 22 and Equations C.9 through C.16.

Table 22: Weld analysis parameters for center horizontal channel.

Description	Variable	Units
Area of weld, treated as a line	A_w	in
Section modulus, of the line	S_w	in ²
Length of channel web	b	in
Length of channel flange	d	in
Shear force	V	lbf
Moment	M	in-lbf
Shear force on weld per length	f_{shear}	lbf/in
Bending force on weld per length	$f_{bending}$	lbf/in
Total force on weld	f_{total}	lbf/in

$$A_w = 40.8 \text{ in} \quad [C.9]$$

$$S_w = bd + \frac{d^2}{6} = 52.9 \text{ in}^2 \quad [C.10]$$

$$V = 13,081 \text{ lbf} \quad [C.11]$$

$$M = 56,246 \text{ ft lbf} = 4,687 \text{ in lbf} \quad [C.12]$$

$$f_{shear} = \frac{V}{A_w} = \frac{13,081 \text{ lbf}}{40.8 \text{ in}} = 321 \frac{\text{lbf}}{\text{in}} \quad [C.13]$$

$$f_{bending} = \frac{M}{S_w} = \frac{4,687 \text{ in lbf}}{52.9 \text{ in}^2} = 88.6 \frac{\text{lbf}}{\text{in}} \quad [C.14]$$

$$f_{total} = \sqrt{f_{shear}^2 + f_{bending}^2} = 333 \frac{\text{lbf}}{\text{in}} \quad [C.15]$$

$$\text{Minimum size of weld} = \frac{f_{total}}{\text{weld strength}} = 0.035 \text{ in} \quad [C.16]$$

Actual size of weld is at least 0.125 inches

The calculations prove the adequacy of the existing welds. A factor of safety of 3.5 is observed under the conservative assumption that the welds are one-eighth inch fillet welds. It consequently follows that the factor of safety for all the other structural members is

higher than 3.5. Additionally, it must be noted that no failures were observed on the structural members which provides strong support that the welds were properly sized according to the original design.

C.5 Finite Element Model Results

ANSYS Workbench, Version 13, was used for the structural finite element analysis (FEA). A SolidWorks model was imported to ANSYS. It was meshed with 127,292 elements, and the stresses and deformation were computed. The maximum stress due to the hydrostatic differential head of five feet was 13.8 ksi and occurred at the center of the bottom horizontal structural channel. Figure 34 and Figure 35 show the general stress levels experienced by the trashrack. Figure 36 shows the deformation due to the differential hydrostatic load.

The structural model was examined without the diagonal tie rods or braces to ensure the trashrack was strong enough without the additional diagonal support.

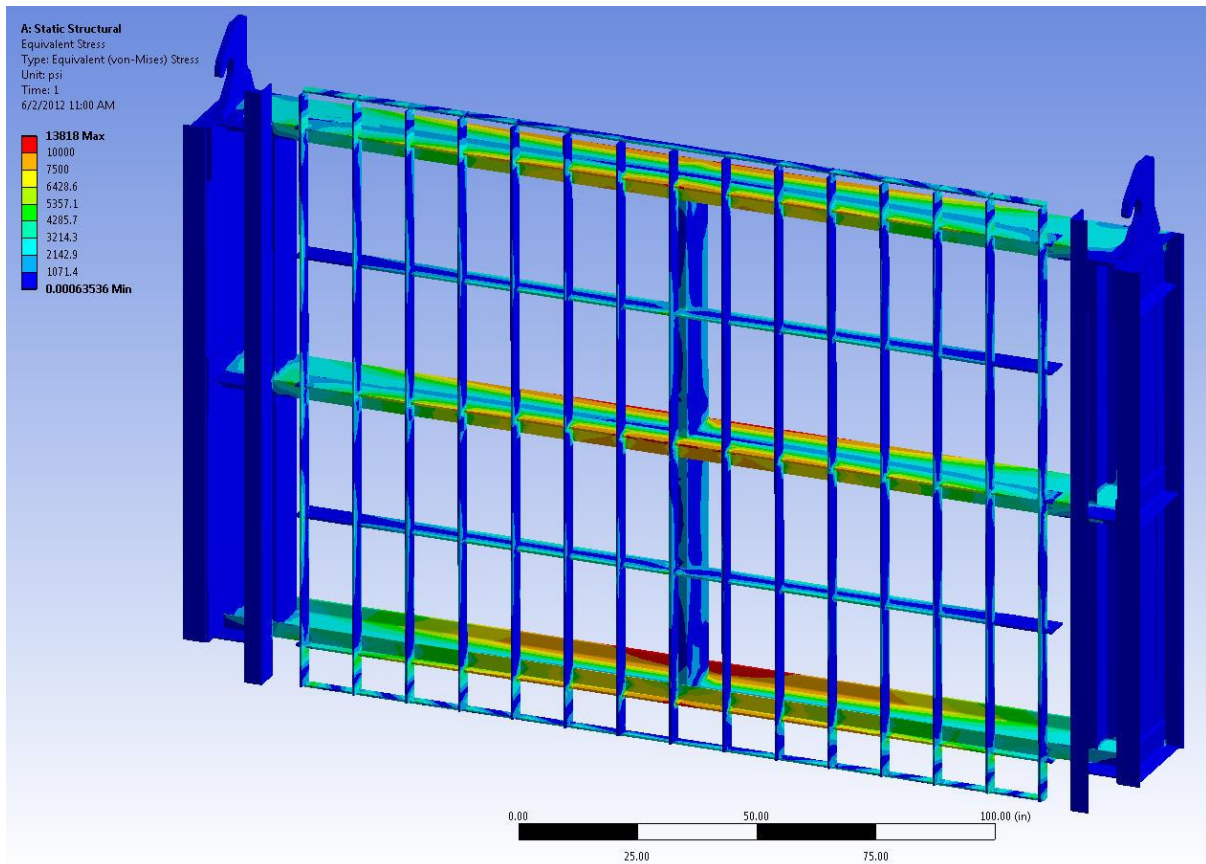


Figure 34: Front view of the trashrack modeled in ANSYS with a differential hydrostatic head of 5 feet. The maximum Von Mises stress is 13.8 ksi.

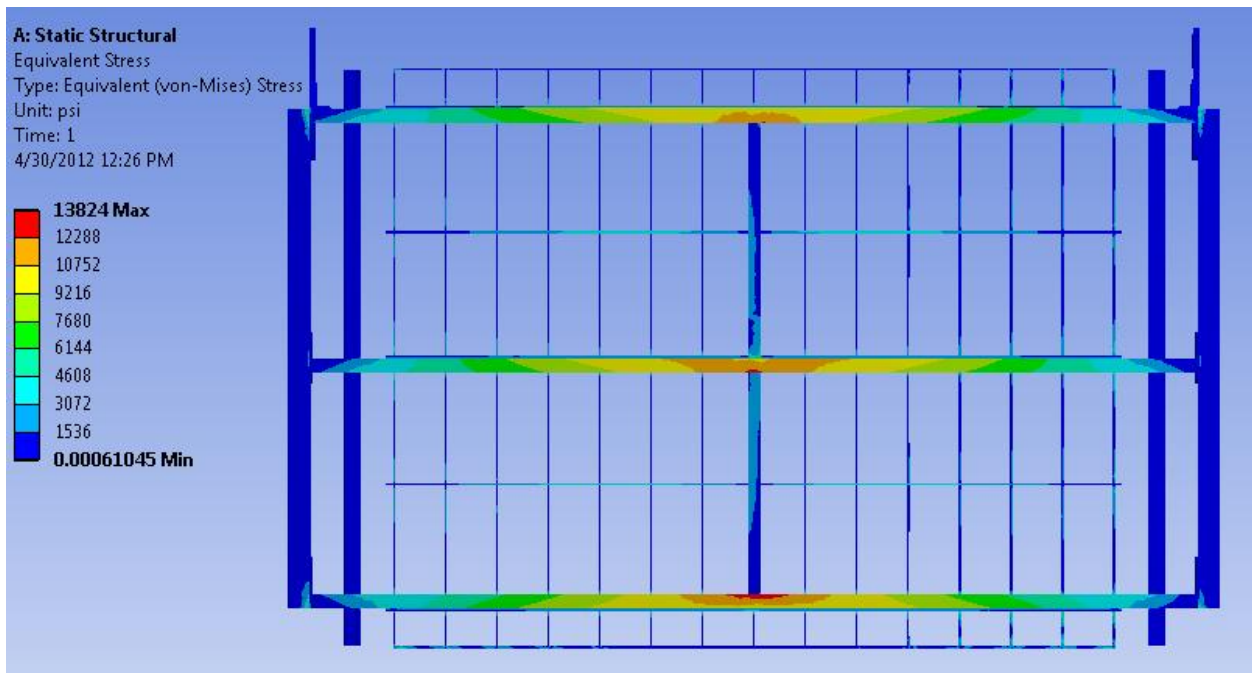


Figure 35: Rear view of the trashrack in ANSYS. The maximum stress (13.8 ksi) occurs at the center of the horizontal structural channels.

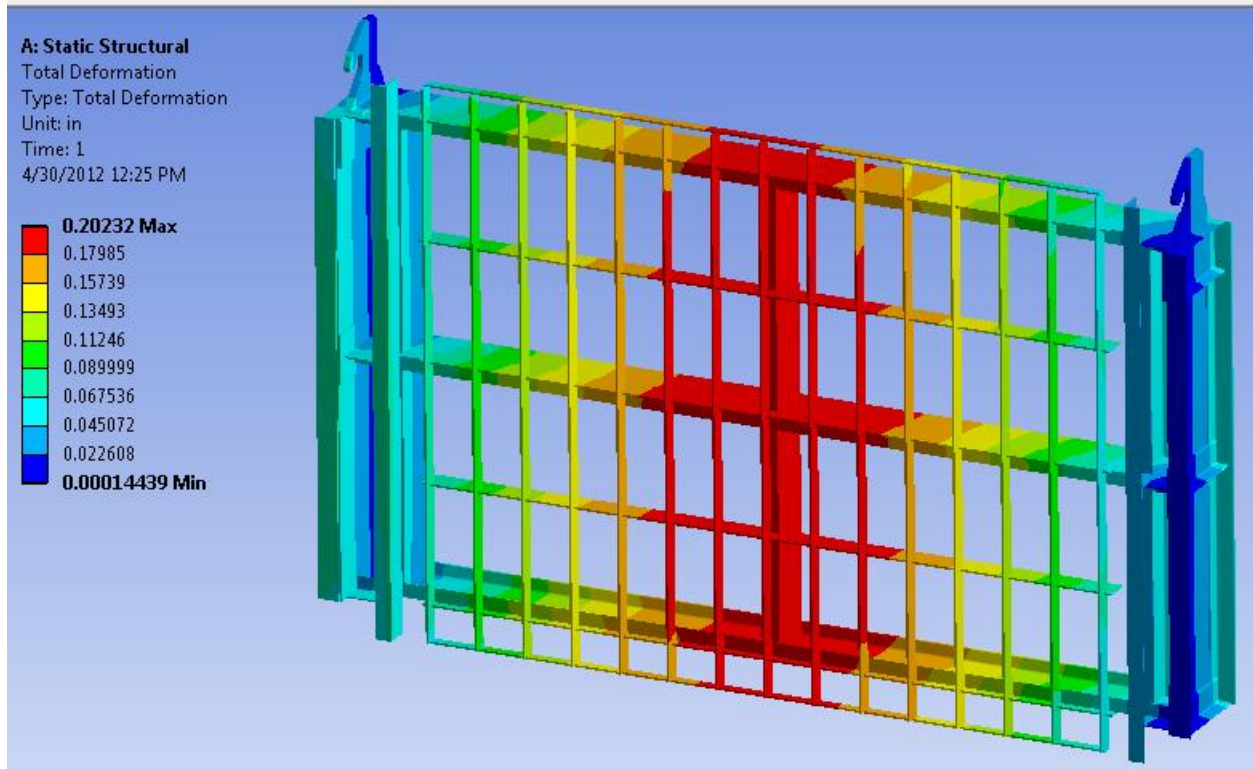


Figure 36: Front view of the trashrack in ANSYS displaying the deformation due to the applied load. The maximum deformation is just over 0.2 inches.

C.6 Tie Rod Replacement Calculations

The structural drag and forcing frequency calculations are provided in this section for the diagonal braces which were recommended to replace the tie rods.

Table 23: Bending and shear stress calculations for the rods and the angle diagonal braces.

Description	Variable	Units	Original 0.875" Rod	1.25" Rod	L2x2x0.375
Coefficient of Drag	C_D	-	1.17	1.17	1.55
Projected length	L	in	108.5	108.5	108.5
Projected width	d	in	0.875	1.25	2.8
Projected area	A	in ²	95	136	304
Water density	ρ	slug/in ³	0.0000143	0.0000143	0.0000143
Water velocity	V	in/s	95.6	95.6	95.6
Drag force	F_D	lbf	7.3	10.4	30.8
Distributed load	w	lbf/in	0.07	0.10	0.28
Moment	M	in-lbf	99	141	418
Distance to neutral axis	c	in	0.4375	0.625	0.89
Radius of gyration	r	in	-	-	0.389
Cross sectional area	A_c	in	0.60	1.23	1.36
Moment of inertia	I	in ³	0.029	0.120	0.206
Shear stress	V	psi	6.0	4.2	11.3
Bending stress	σ	psi	1498	734	1806

Table 24: Vortex shedding frequency according to the Strouhal number.

Description	Variable	Units	Original 0.875" Rod	1.25" Rod	L2x2x0.375
Strouhal number	-	-	0.2	0.2	0.175
Water velocity	V	in/s	95.6	95.6	95.6
Projected width	d	in/s	0.875	1.25	2.8
Vortex shedding frequency	f	Hz	21.9	15.3	6.0

Appendix D: Chelan PUD Painting Specifications

Chelan County PUD has a 23 page document outlining the painting specifications for all rehabilitation projects at Rock Island Dam. Since it was first used for a contract in 2004, it has been refined to define the surface preparation and painting procedure for an array of applications. Section 3.16.1 of the painting specifications document, shown as an excerpt on the next page, classifies the necessary sandblasting operation, type of paint, and thickness of application for metals submerged in water. It clarifies that two coats of coal tar epoxy are to be applied to the trashracks to a thickness of 24 mils after sandblasting to near white metal (SP 10).

Handle coated items with care during loading/unloading, installation, and erection operations to minimize damage. Do not place or store coated items on the ground or on top of other work unless ground or work is covered with a protective covering or tarpaulin. Place coated items above the ground upon platforms, skids, or other supports.

Cover coated items one-hundred percent (100%) with protective coverings or tarpaulins to prevent deposition of road salts, fuel residue, and other contaminants in transit.

3.16 PROTECTIVE COATINGS SYSTEM SCHEDULE

3.16.1 System No. 1 - Water Passage Submerged Metal

Apply to the following ferrous items:

1. Headcovers, Runner Hub, Runner Nose Cone, Stay Ring/Vanes, Wicket Gates, Discharge Liner and Draft Tube Liner

Surface Prep.	Paint Material	Min. Coats, Cover
Abrasive Blast, (SP 10)	Coal Tar Epoxy	1 or 2 coats as needed to achieve 24 mils DFT total

3.16.2 System No.2 - Metals in Contact with Water

Shop or field apply this system to all surfaces exposed to water. Also apply to the following items or areas in the field at the project site:

1. All turbine pit components such as operating ring, links, levers, walks, turbine pit wall, inside of all headcovers, etc.
2. Steel Pipe, Plate, Fittings, and Miscellaneous Metals

Surface Prep.	Paint Material	Min. Coats, Cover
Abrasive Blast, (SP 10)	High Build Epoxy Primer (Aluminum filled)	1 coat, 6 MDFT
	Epoxy Top Coat	1 coat, 6 MDFT Total 12 MDFT

Note: Solvent Clean (SP1) and Power Tool Clean (SP 3) areas for spot repairs of shop-applied lining in accordance with paint manufacturer's recommendations.

3.16.3 System No. 3 - Metal Exposed to Atmosphere

Shop or field apply this system to all atmospheric exposed metal surfaces and the following items or areas:

1. The exterior of carbon steel pipe, plate, and miscellaneous metals not in contact with water or soil.

Appendix E: Additional Pictures

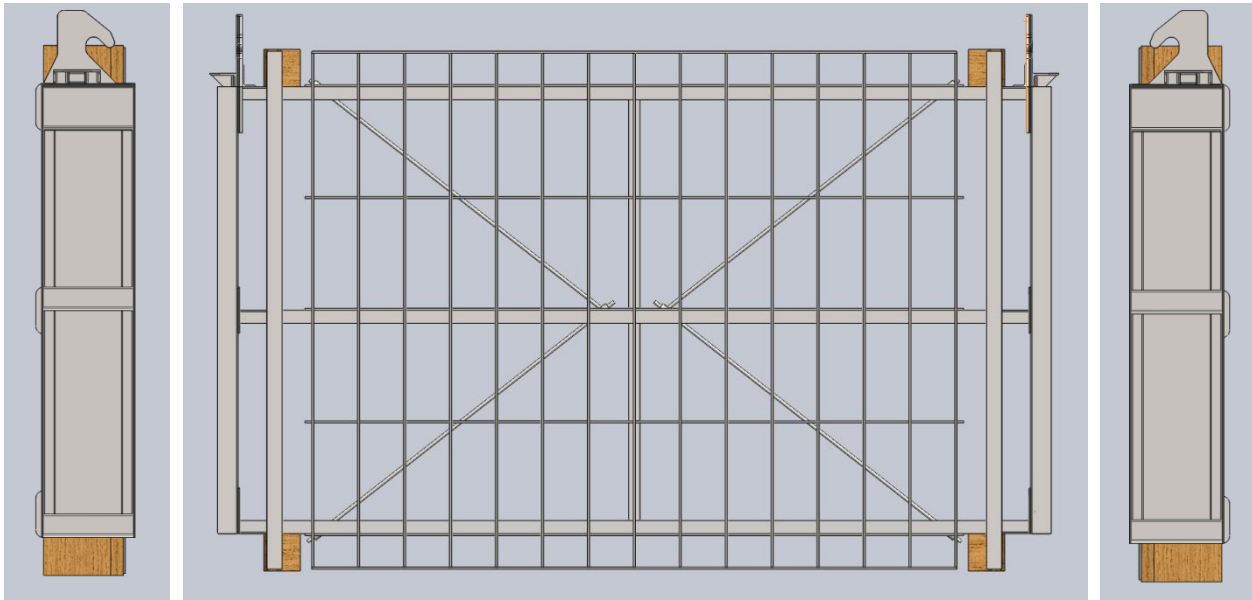


Figure 37: Front and side views of original trashrack model.

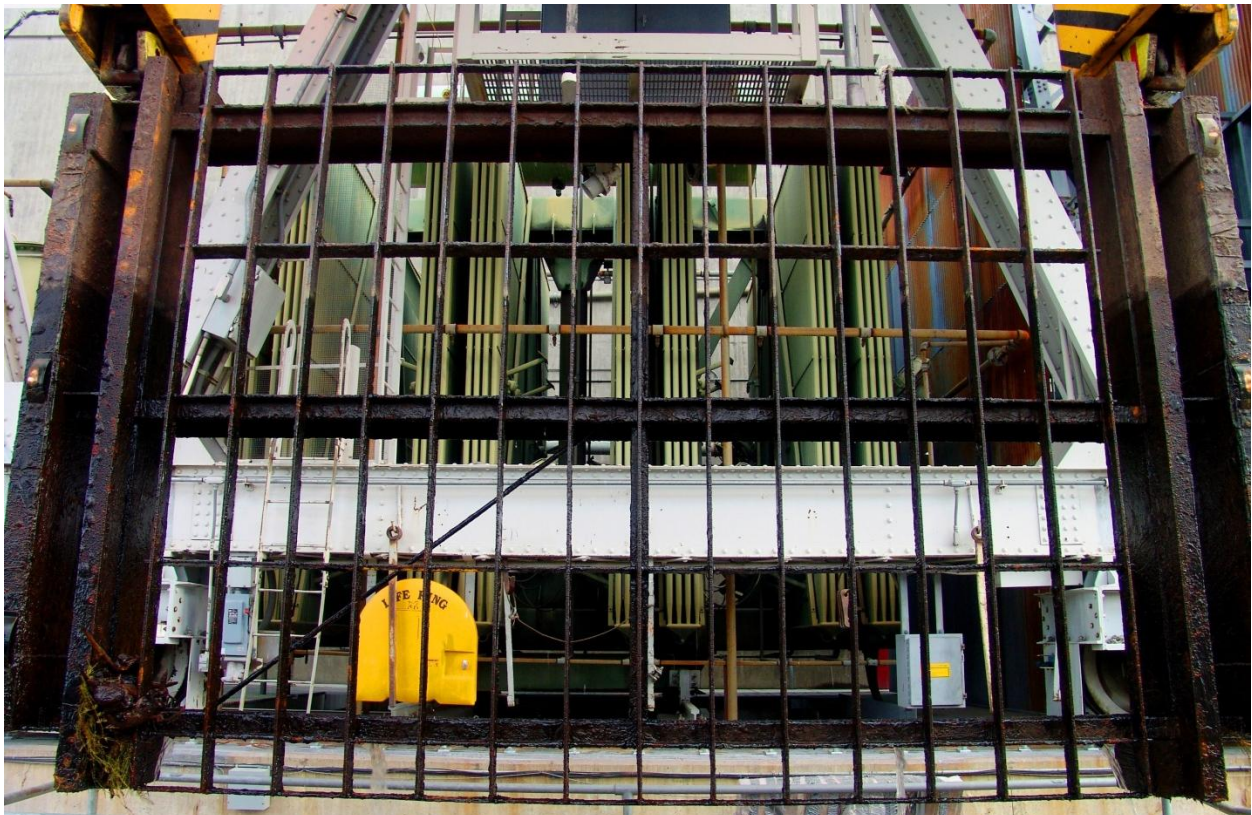


Figure 38: Front view of the original trashrack with steel rackbars while hanging from the gantry crane. Three of the four diagonal tie rods are missing.



Figure 39: Front view of a original trashrack with wood rackbars. The structural supports and diagonal tie rods are identical for the wood rackbar and steel rackbar trashracks.



Figure 40: Rehabilitated trashrack demonstrating the new diagonal braces. The angle iron braces were installed with the elbow of the angle pointing directly into the flow.



Figure 41: Rehabilitated trashrack. The new diagonal braces were installed and the structure was sandblasted and painted black. Tim Scheumann is standing in front of the trashrack.

This page was intentionally left blank